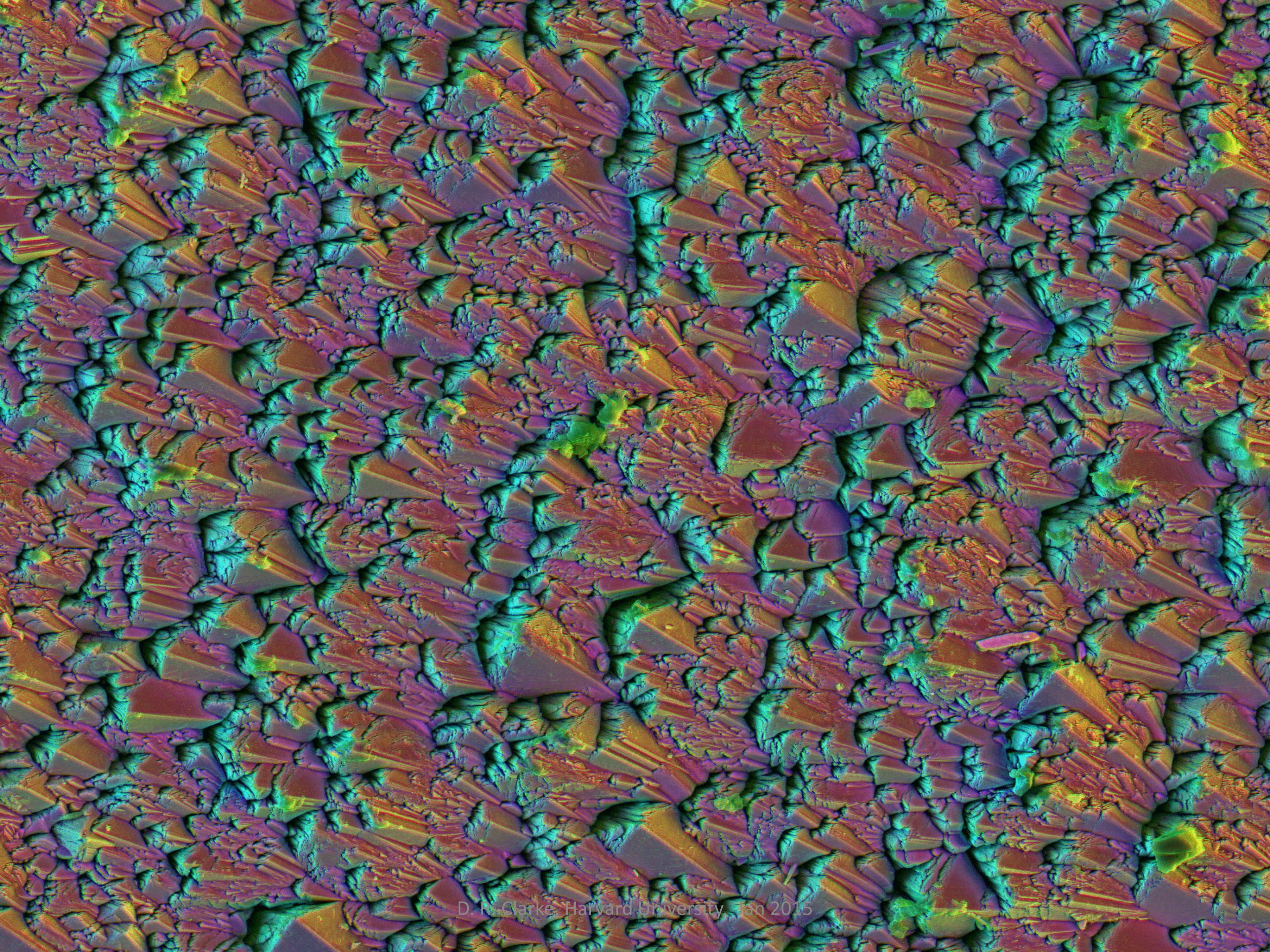
D. R. Clarke, Harvard University, Jan 2015

HARVARD
School of Engineering
and Applied Sciences

James Mueller Lecture:

"Thermal Barrier Coatings for Gas Turbines"

Materials Discovery and Applications Group

David R. Clarke

clarke@seas.harvard.edu

Gas Turbines

Schematic

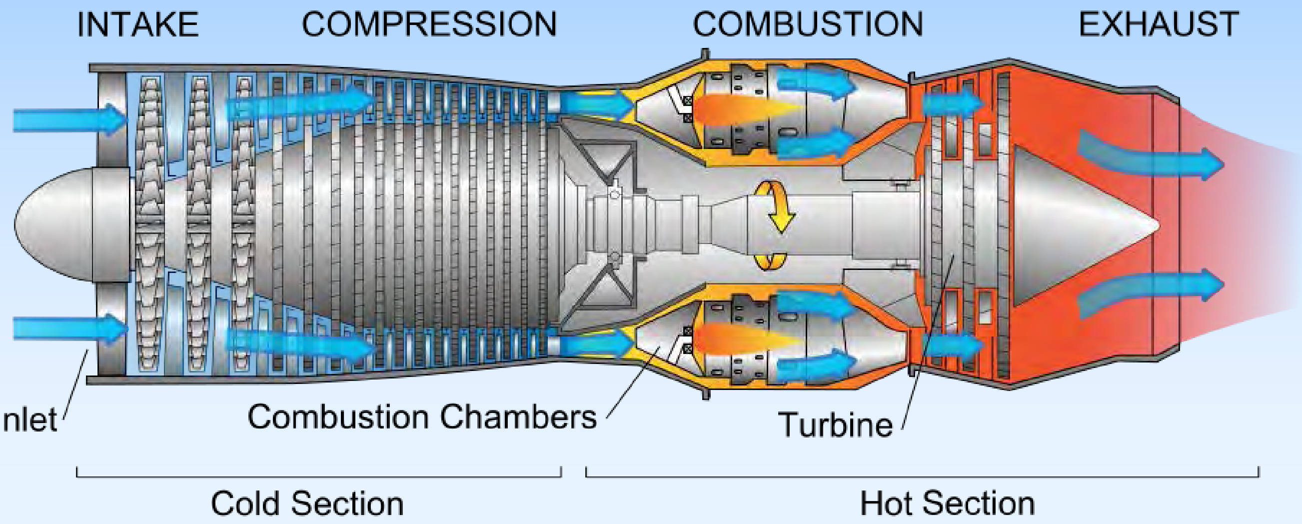

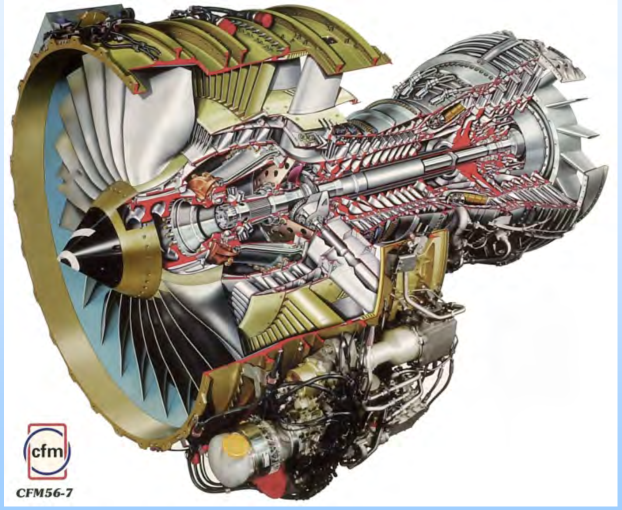

Siemens Power Generation
340 MWe

Fuel Efficiency in the Aeroturbine Industry

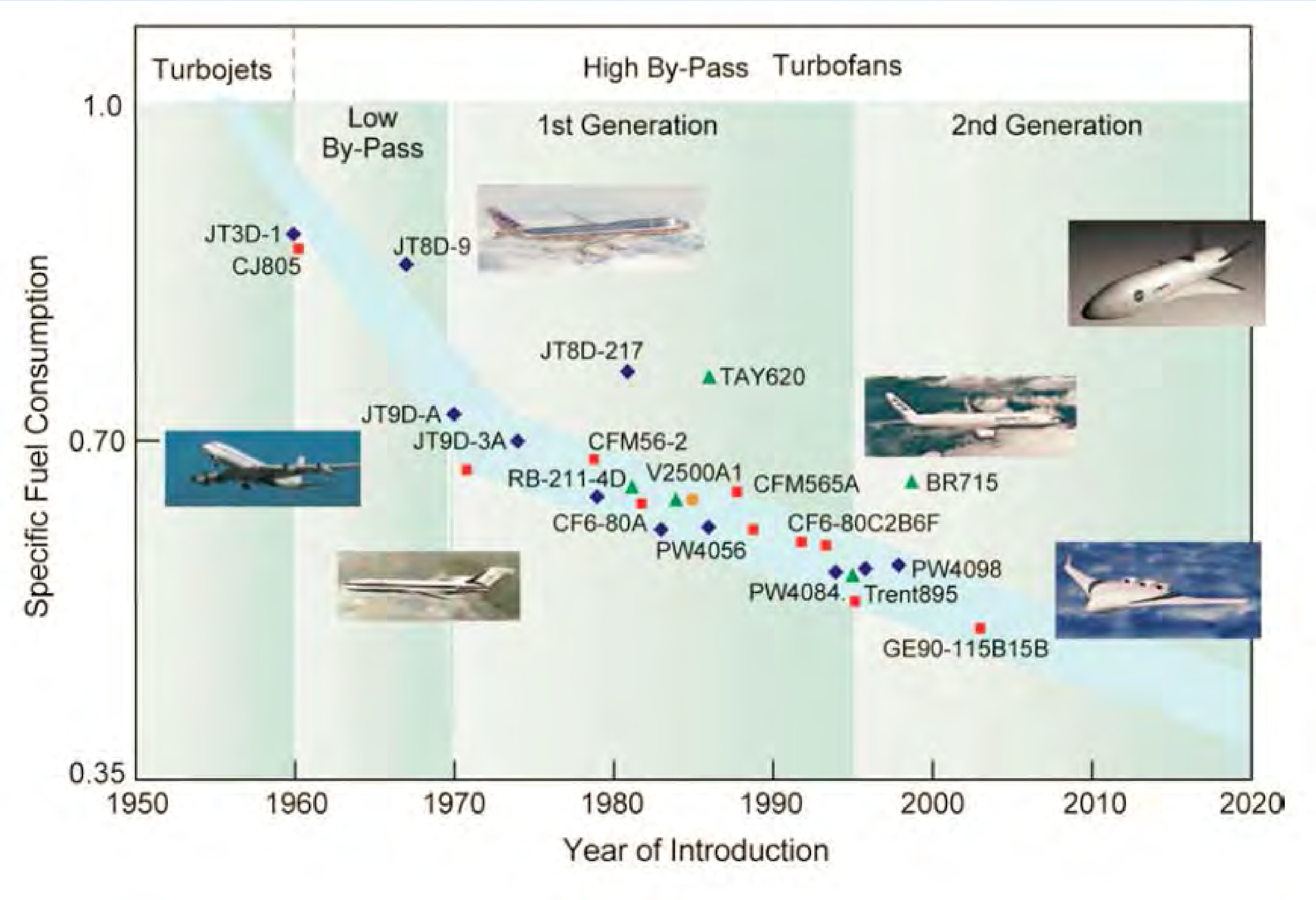

D. R. Clarke, Harvard University, Jan 2015

Gas Turbines Offer High Power Densities and Route to Quickly Displace Coal

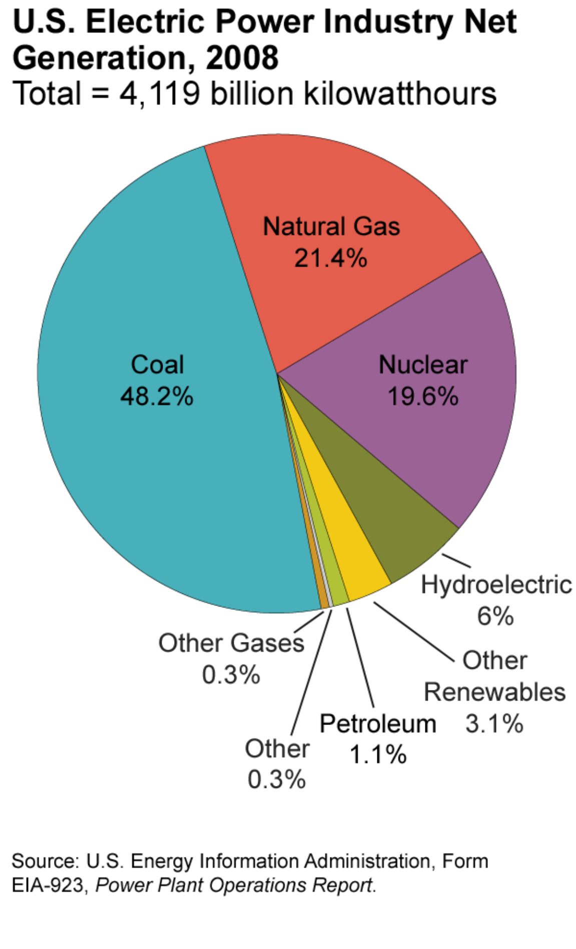

50 MWe GE. LM6000

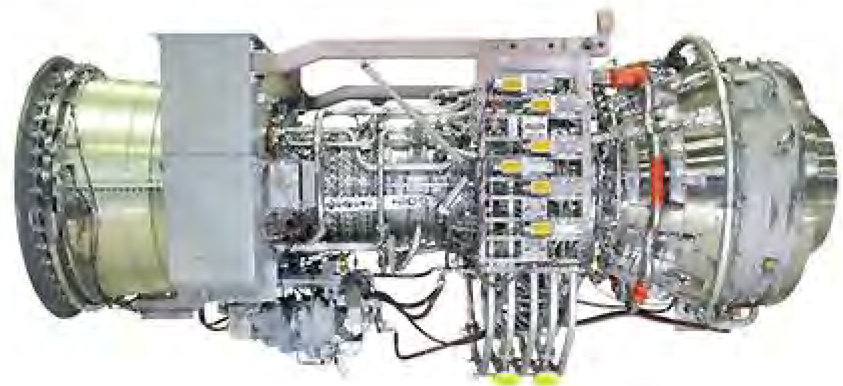

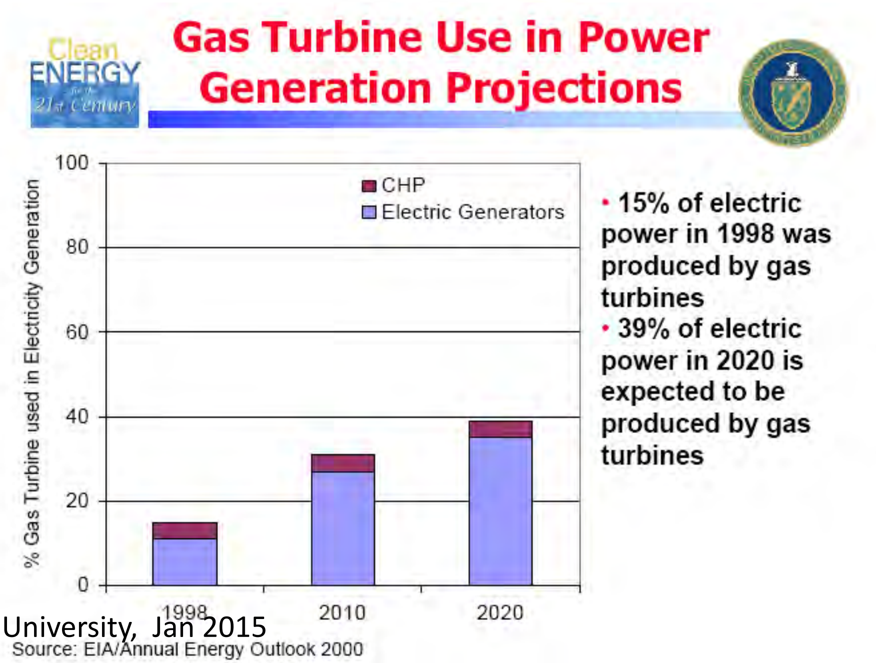

Replacing coal with natural gas turbines decreases CO_2, Hg, radioactive and dust emissions, and is also more energy efficient.

What 1% Improvement in Gas Turbines Could Buy Us

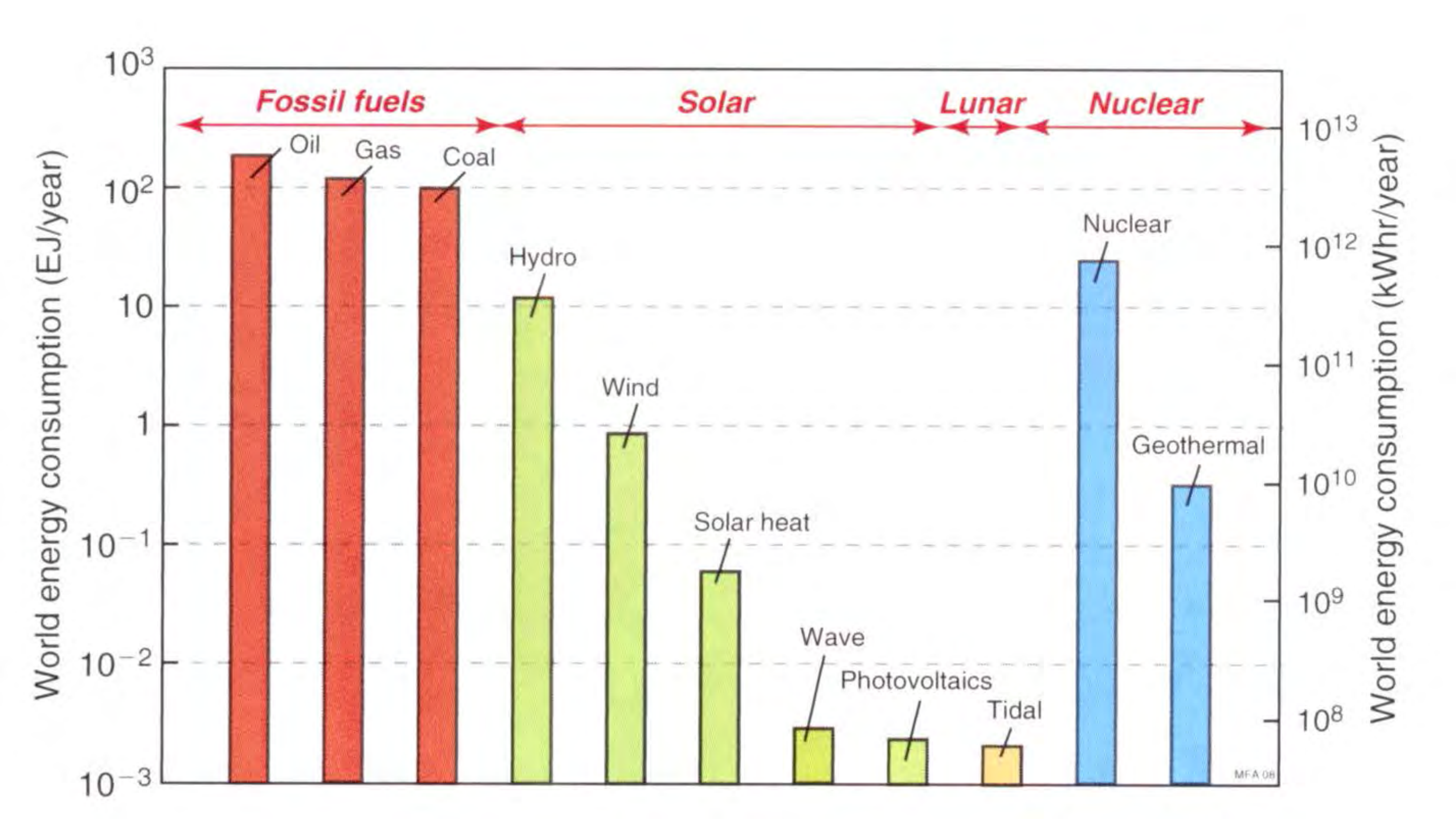

2009 data

Ashby, Materials and the Environment, Elsevier

NB. 30% of natural gas is used to produce electricity. 1% improvement > all renewables

Output Power Depends on Turbine Inlet (T4) Temperature

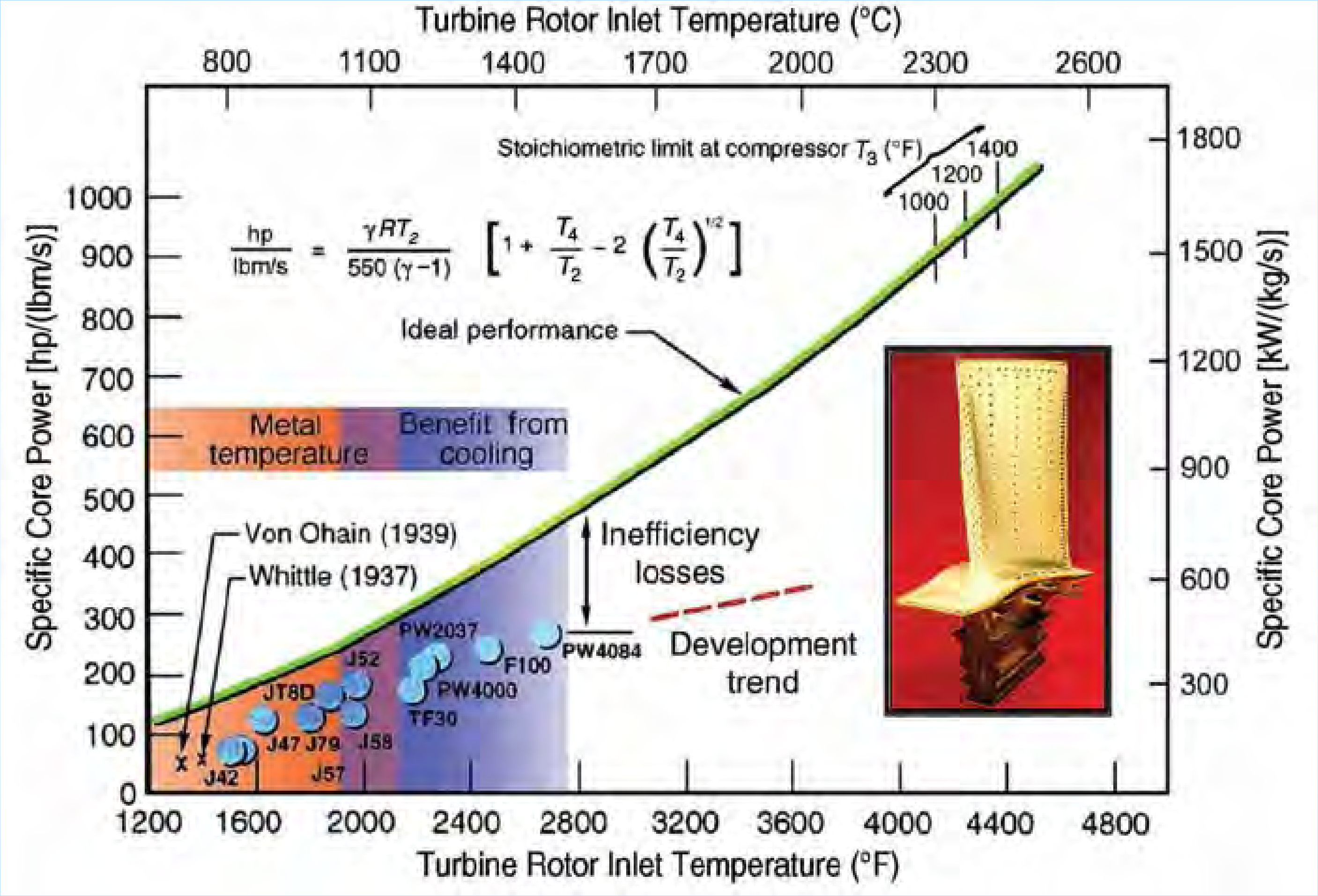

Dimiduk and Perepezko, MRS Bull 639 2003

Increase in Turbine (T4) Temperatures over Fifty Years

Yttria-stabilized
zirconia coatings
~ 150 – 500 micron thick

Thermal gradient
~ 150-200 K/mm

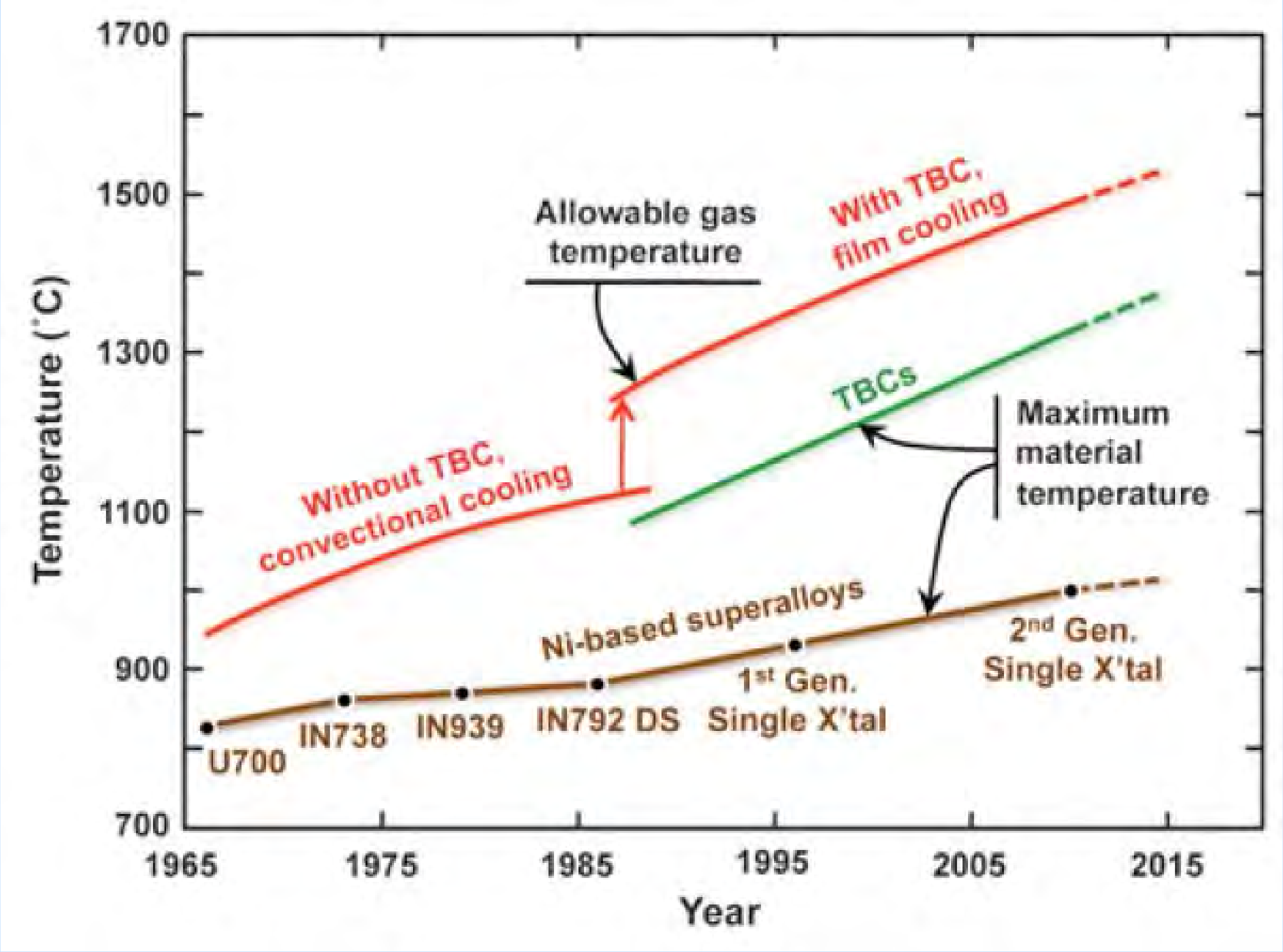

Thermal barrier coatings have enabled a jump
in turbine temperatures and energy efficiencies

D. R. Clarke, Harvard University, Jan 2015

Thermal Conductivity of Oxides

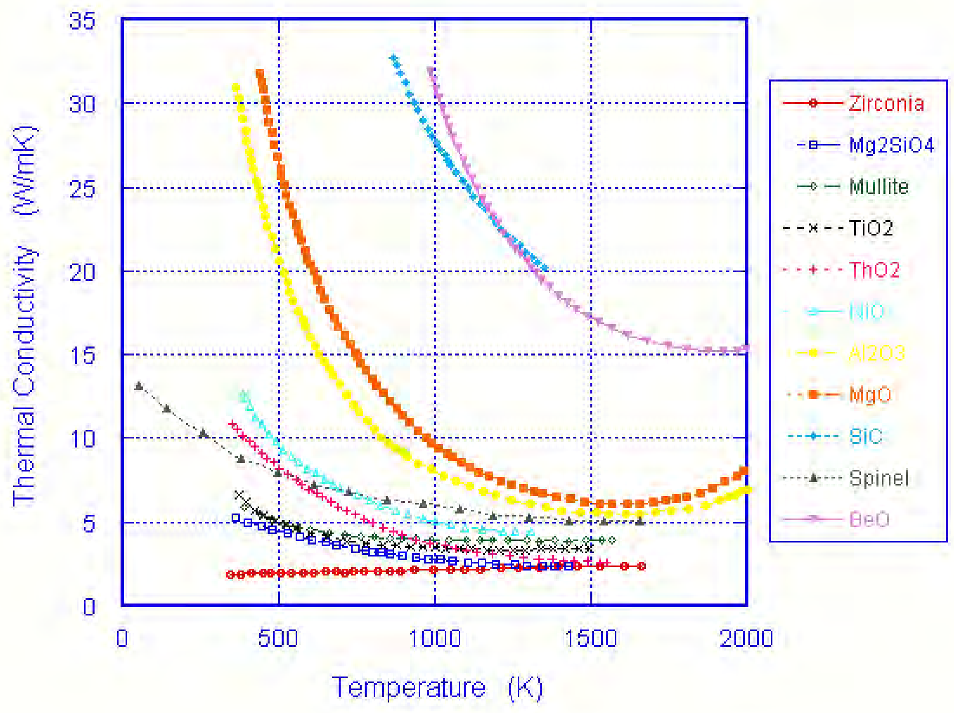

Kingery et al, ca 1955

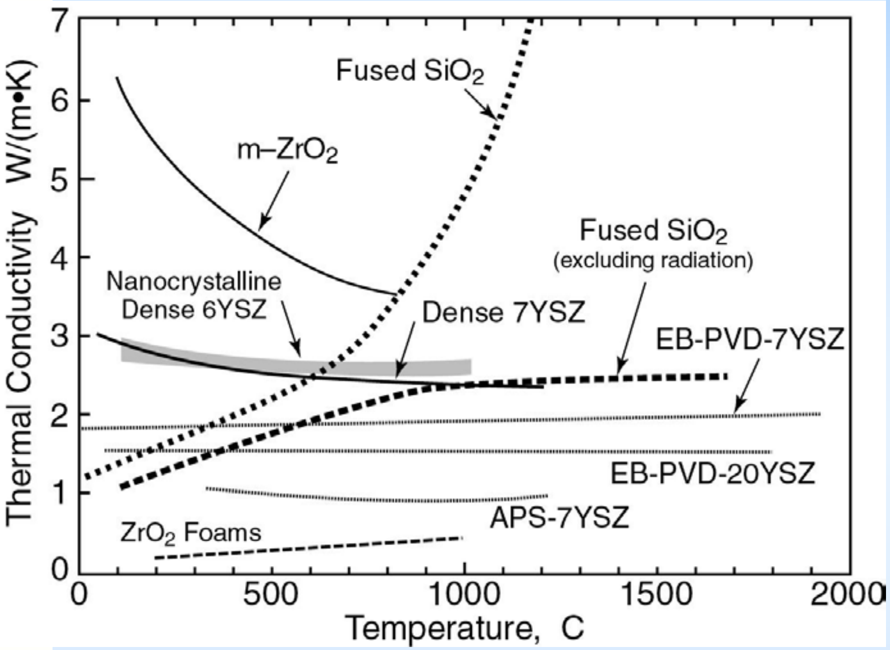

Zirconias -- Levi

Thermal conductivity asymptotes to a minimum value at high temperatures

The Minimum Thermal Conductivity

Approach:

Adopt Debye equation and express it's high-temperature limit in terms of measurable physical parameters.

$$\kappa \to \kappa_{\min} \quad ; \quad \kappa = C_V\, v_m \Lambda / 3 \to k_B v_m \Lambda_{\min}$$

Dulong-Petit equation: $C_V \to 3k_B$ as $T > \Theta_D$

$$\Lambda_{\min} \to \left(\frac{M}{\rho\, m N_A} \right)^{1/3}$$

Cube root of atom volume

Mean phonon velocity: $v_m = 3^{1/3} \left(\frac{1}{v_p^3} + \frac{2}{v_S^3} \right)^{-1/3}$

Over wide range of Poisson ratio: $v_m = A\sqrt{\frac{E}{\rho}}$

$$A = 0.87 \pm 0.02$$

Combining these approximations:

$$\kappa_{\min} \to 0.87 k_B N_A^{2/3} \frac{m^{2/3} \rho^{1/6} E^{1/2}}{M^{2/3}}$$

$$\Theta_D = 3.39 \frac{\hbar}{k_B} N_A^{1/3} \frac{m^{1/3} E^{1/2}}{M^{1/3} \rho^{1/6}}$$

In terms of atomic volume

$$\kappa_{\min} = k_B\, v_m\, \Lambda_{\min} \to 0.87 k_B \overline{\Omega}_a^{-2/3} (E/\rho)^{1/2}$$

High-Temperature Thermal Conductivity Scaling

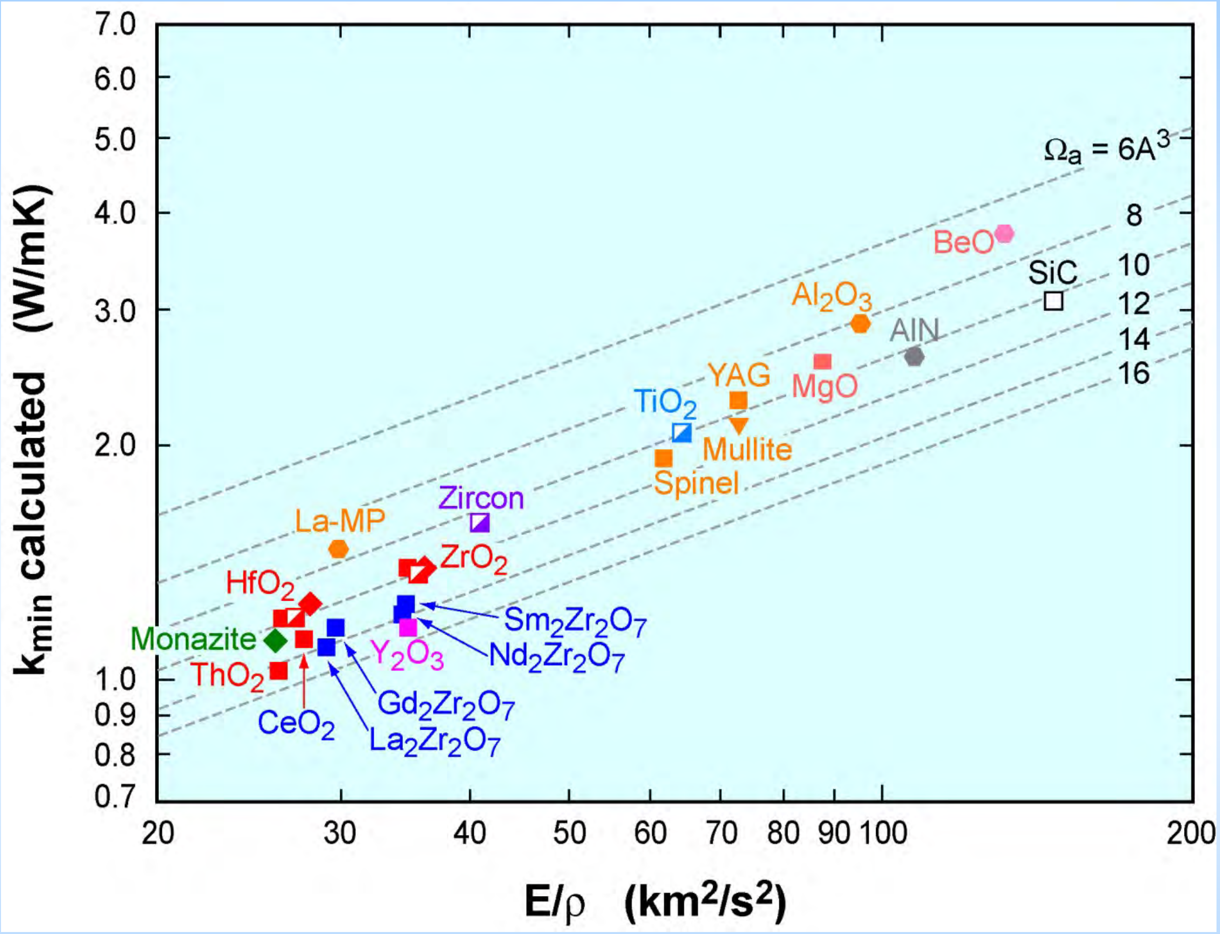

$$\kappa_{\min} = k_B\, v_m\, \Lambda_{\min} \rightarrow 0.87 k_B\, \overline{\Omega}_a^{\,-2/3} \left(E/\rho\right)^{1/2}$$

$$\overline{\Omega}_a = \left[M / \left(m\,\rho\, N_A\right)\right]$$

D. R. Clarke, Harvard University, Jan 2015

Oxides with Low Conductivity Discovered in Last Decade

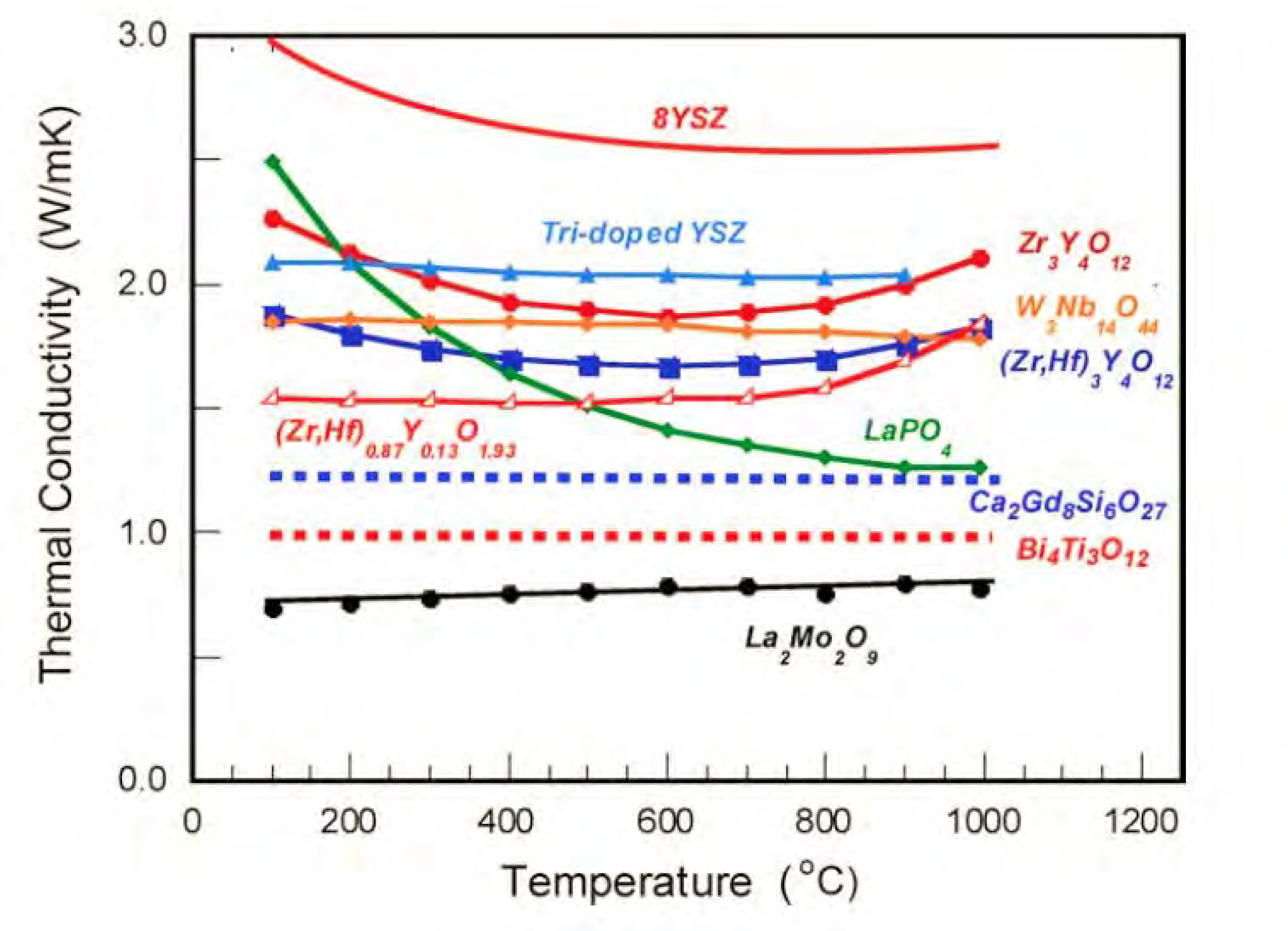

Examples of Grain Size Effect

SrTiO3

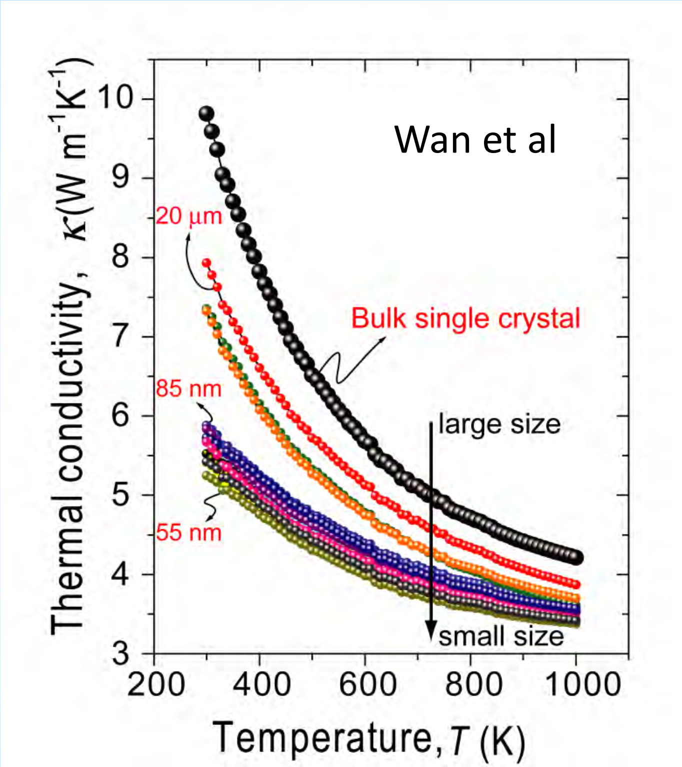

Tetragonal zirconia

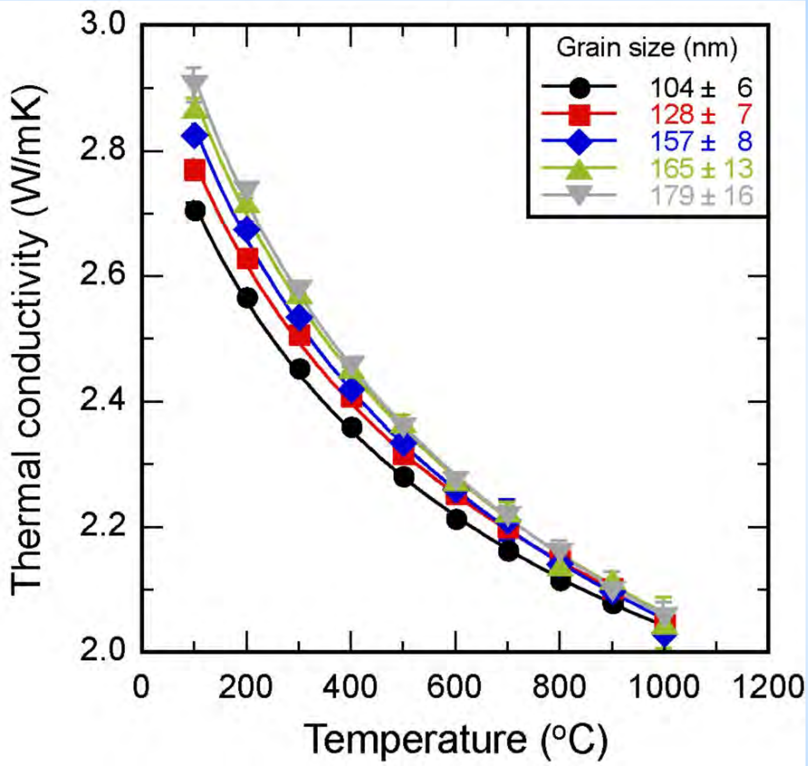

Grain size effect on thermal conductivity can be significant at low temperatures but decreases with increasing temperatures until at highest temperatures there is little or no effect

The Y-Ta-Zr-O System

Y-doped ZrO_2

Meta-stable tetragonal (*t'*) 7YSZ
- Low Y : *t'* -> monoclinic
- High Y : *t'* -> cubic

$YTaO_4$-doped ZrO_2

Transformable (t -> m)

Non-transformable tetragonal
Fracture toughness increases with increasing YTO_4

Lower thermal conductivity than 7YSZ, but no ferroelastic toughening at high temperature

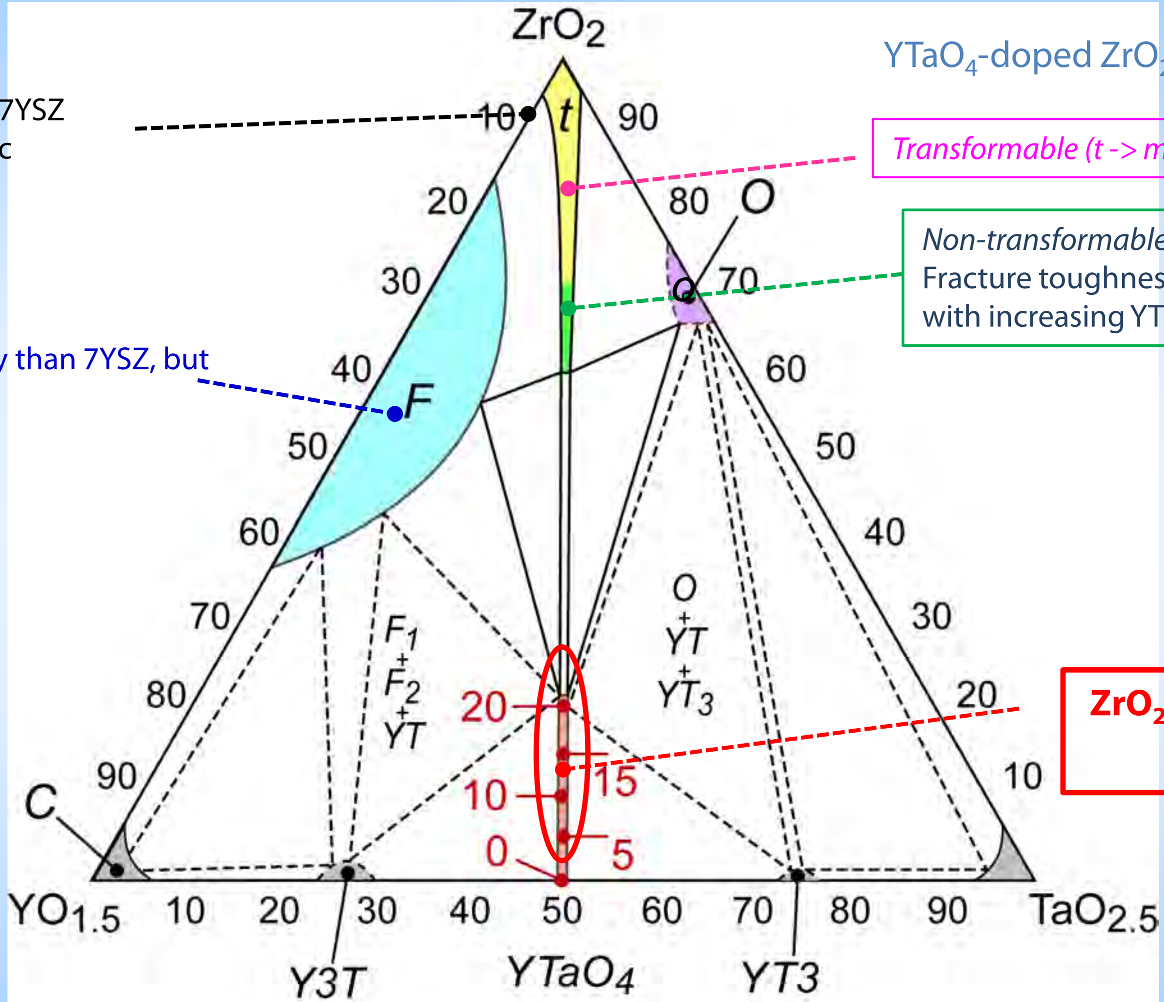

ZrO_2 solid solution In $YTaO_4$

High temperature M-T in $YTaO_4$

F = fluorite (cubic)
O = orthorhombic
t = tetragonal

Pitek and Levi, Surf. & Coatings Tech. 201 (2007) 6044-6050
Phase diagram : Leckie et al. 2010

D. R. Clarke, Harvard University, Jan 2015

The ZrO_2 – $YTaO_4$ Pseudo-Binary

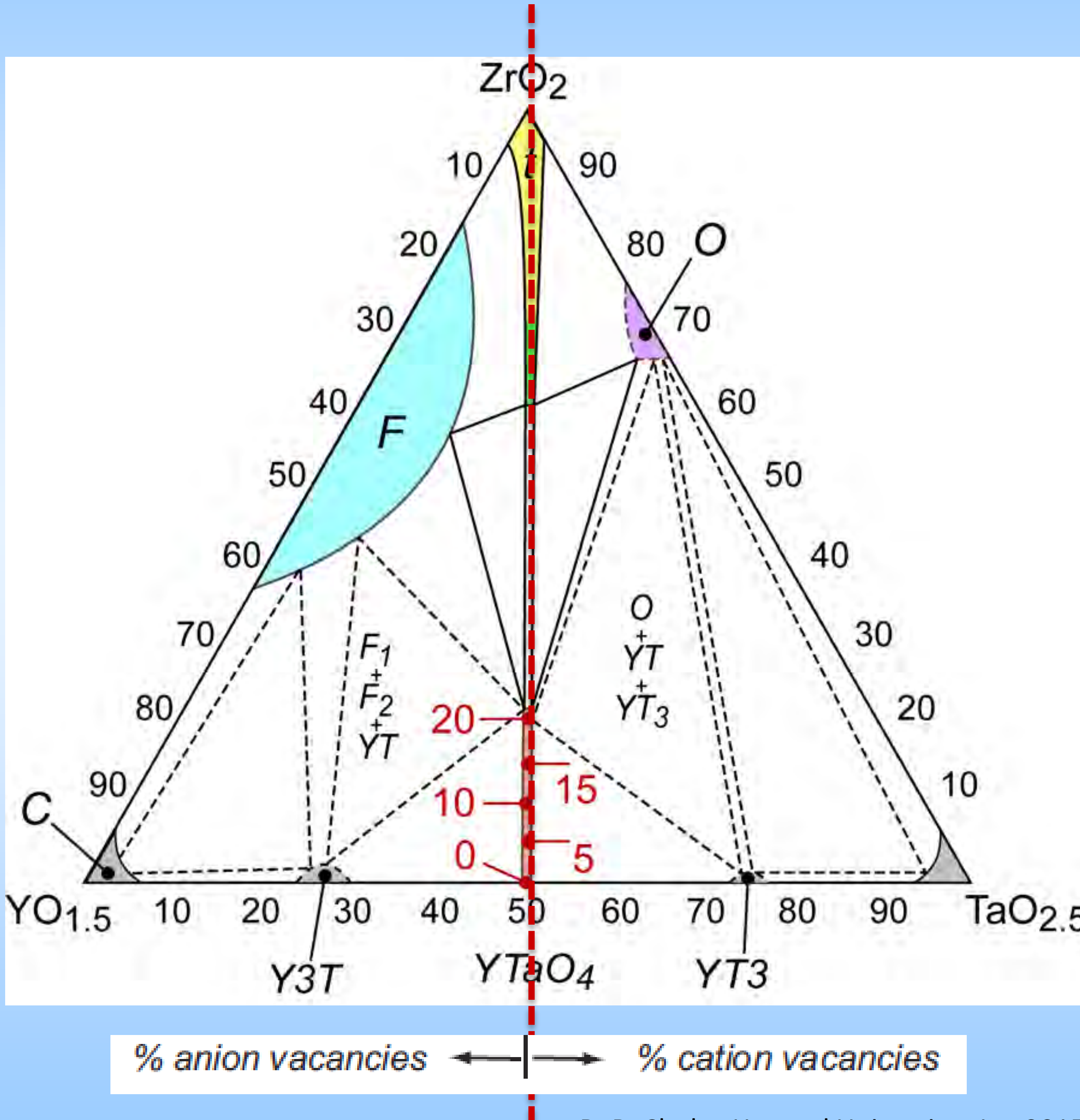

Particular interest in compositions along ZrO_2-$YTaO_4$ Binary

$Y^{3+}_{1-x}Ta^{5+}_{1-x}Zr^{4+}_{2x}O^{2-}_{2}$ compositions do not require structural vacancies to be stable.

Consequently, no conductivity decrease by oxygen vacancies is possible.

D. R. Clarke, Harvard University, Jan 2015

Multi-phase Yttria-Tantala-Zirconia with Low Thermal Conductivity

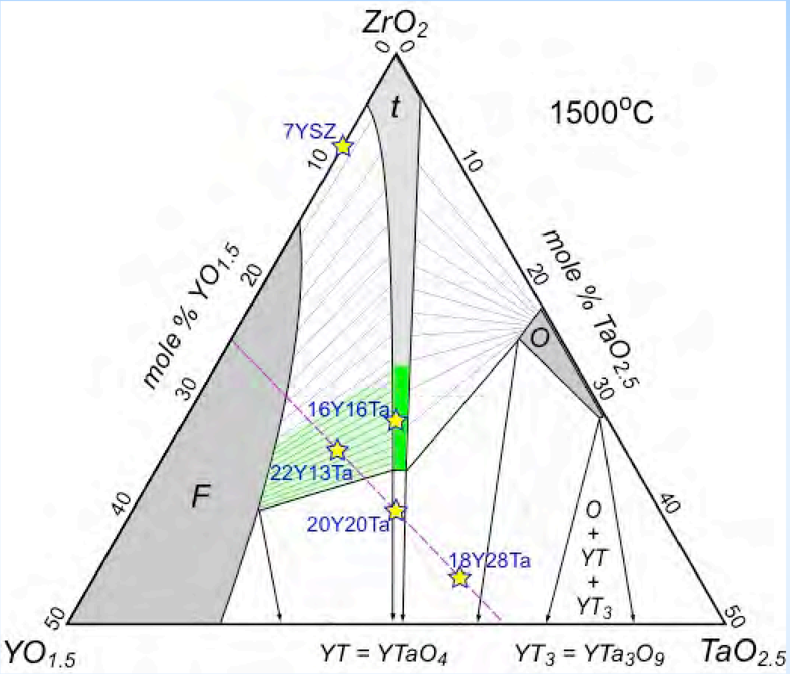

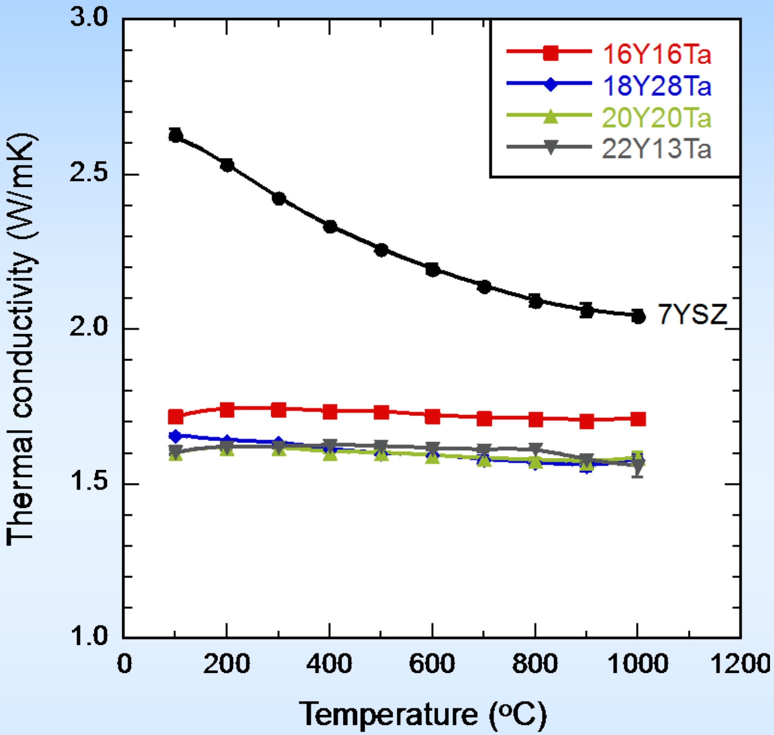

D. R. Clarke, Harvard University, Jan 2015

Variation of Thermal Conductivity with Composition

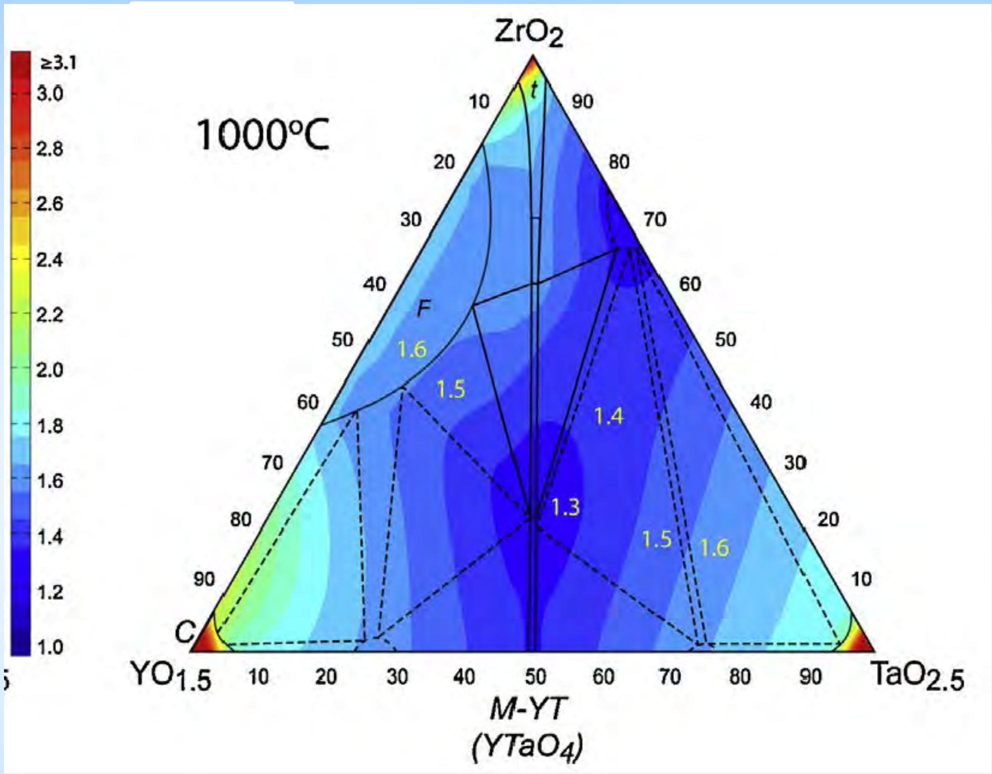

Limarga et al, J Euro. Ceram Soc, 2014

Obtained by interpolation from conductivity measured at different compositions

Phase Transformations in $(Y,Ta)_{1-x}Zr_xO_{4-2x}$

- $YTaO_4$ undergoes *reversible* phase transformation, *m – t*, in which is, evidently, ferroelastic, involving atomic displacement and twinning, and maybe useful as a high temperature toughening mechanism.
- Effect of ZrO_2 solid solution in $YTaO_4$:
  - Stabilizes the tetragonal phases, decreasing the *t-m* transformation temperature and increasing the fraction of non-transformable tetragonal phases retained at room temperature
  - Solid solution creates mass disorder that decreases the phonon mean free path. Evident in:
    - the increase in Raman peaks width
    - the decrease in thermal conductivity
  - Suppresses grain growth
  - Lower thermal conductivity

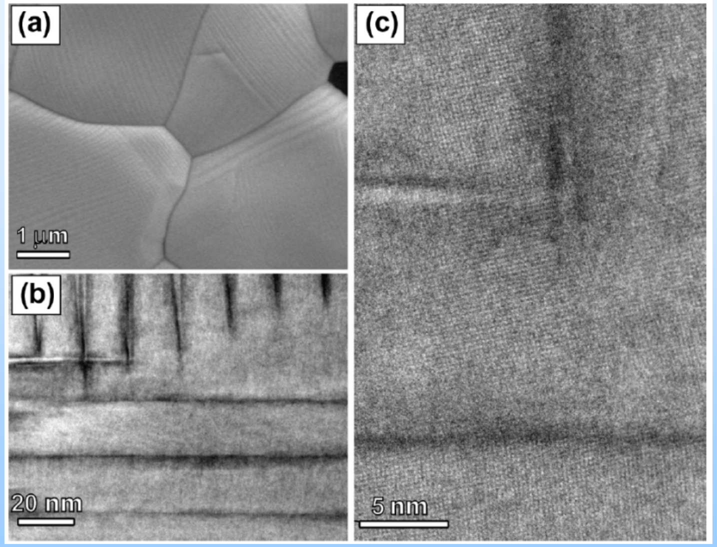

Phase Transformation in $YTaO_4$: Effect of ZrO_2

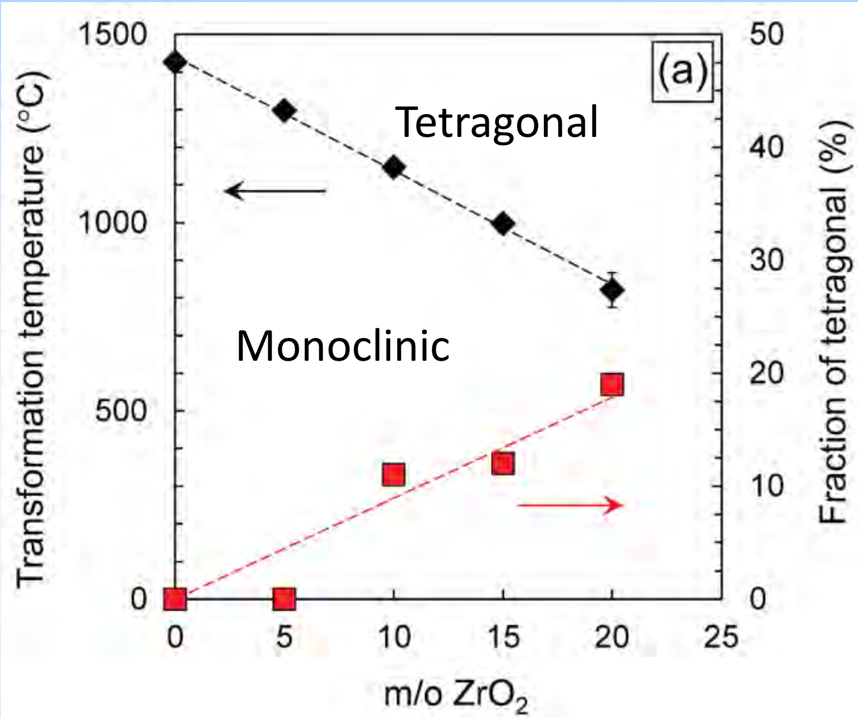

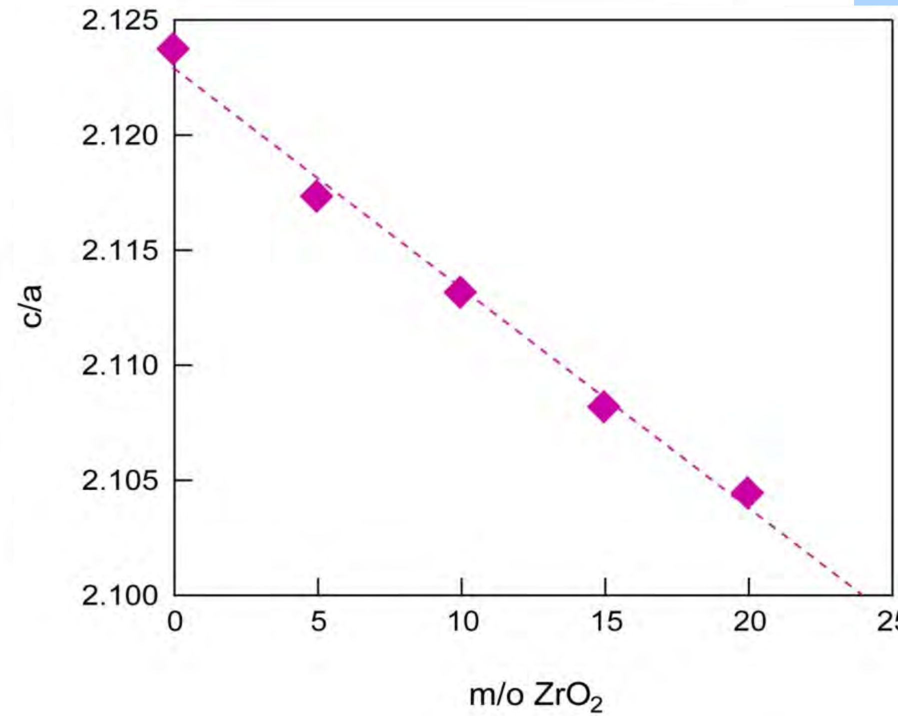

NB. Some tetragonal retained

Zr^{4+} Stabilizes the high-temperature Tetragonal Phase

The Thermal Management Challenge

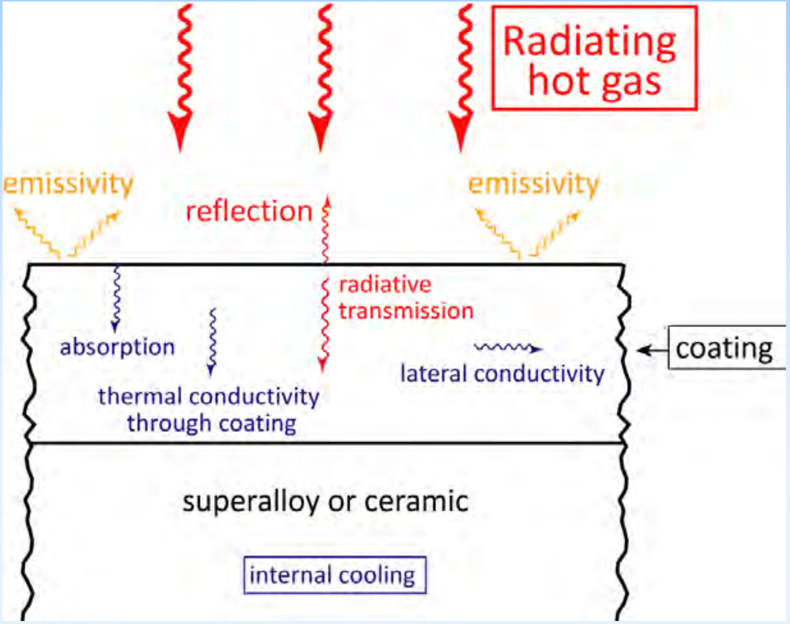

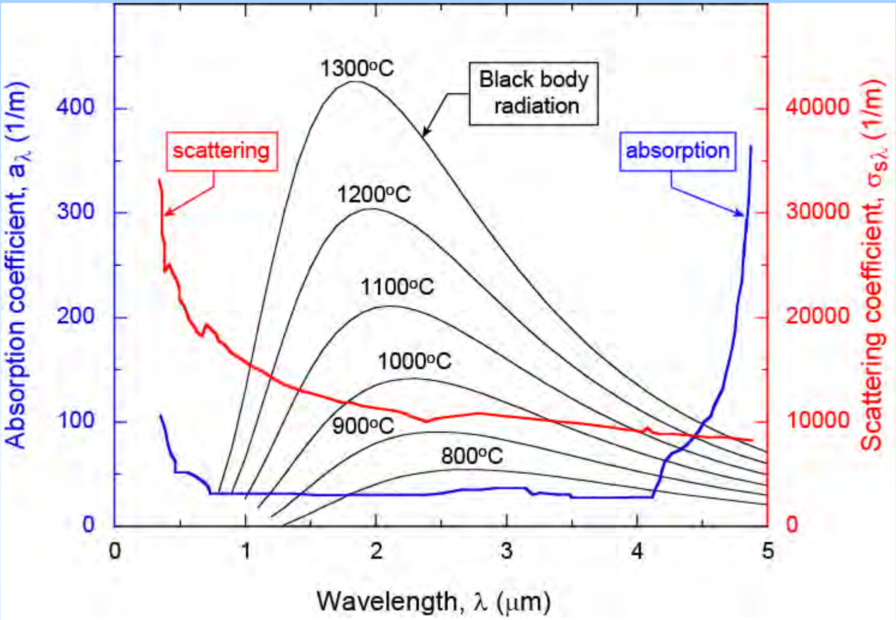

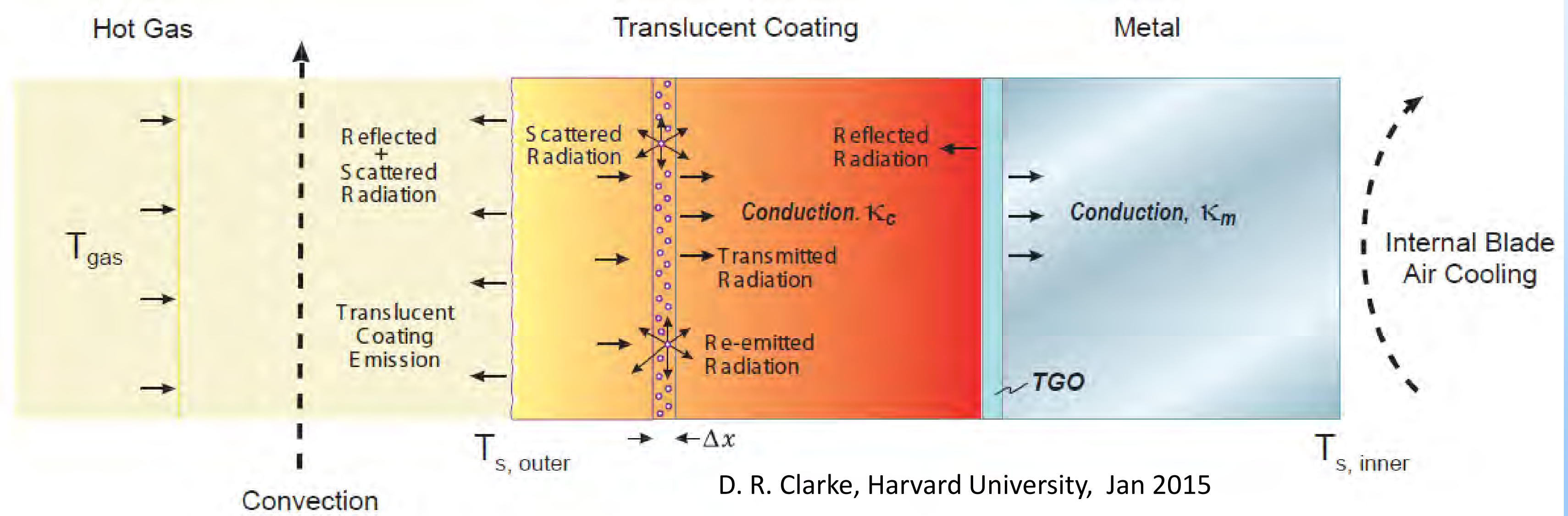

D. R. Clarke, Harvard University, Jan 2015

Porosity Reduces Conductivity and Scatters Thermal Radiation

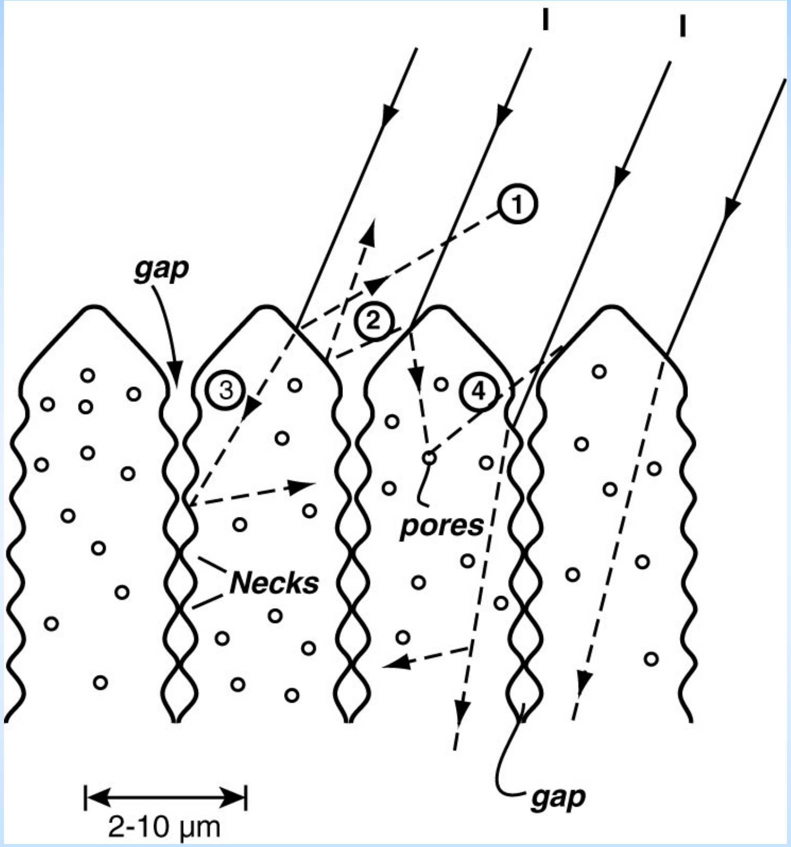

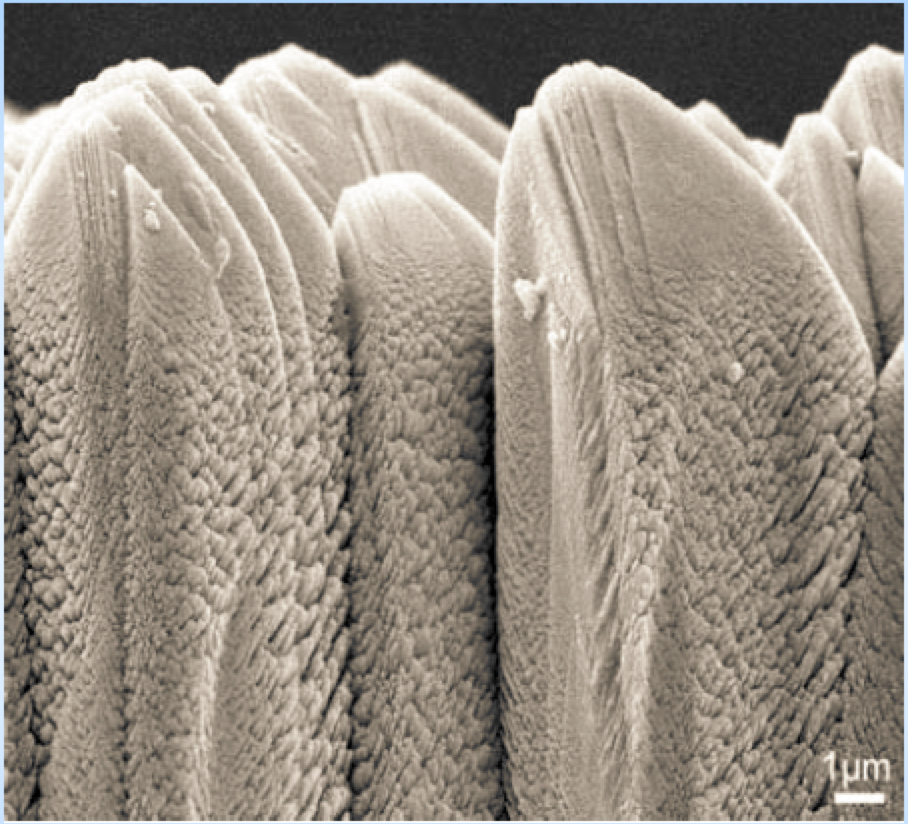

Temperature Distribution For Different Coating Designs

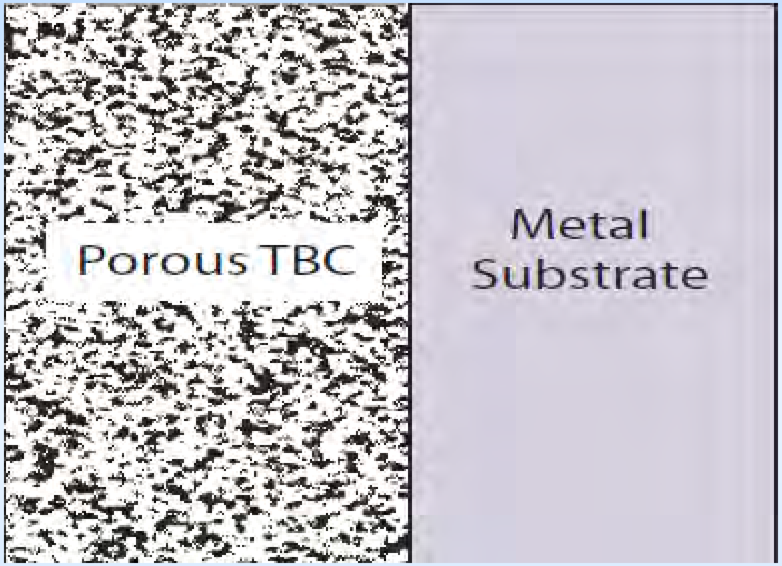

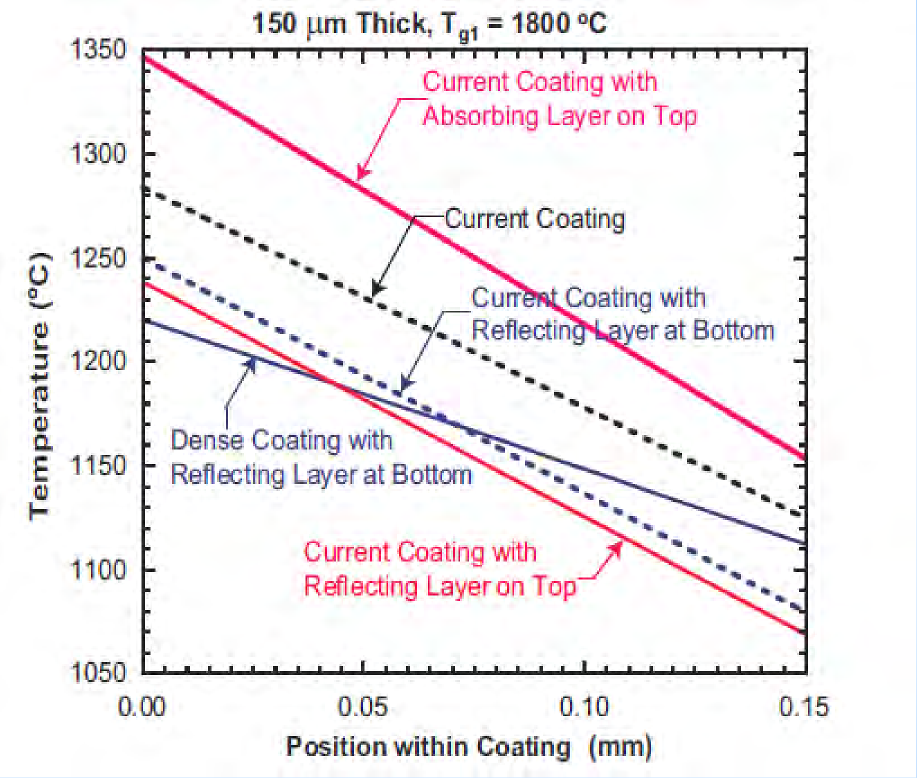

Liguo Chen, Phd Thesis

Temperature Distribution For Different Coating Designs

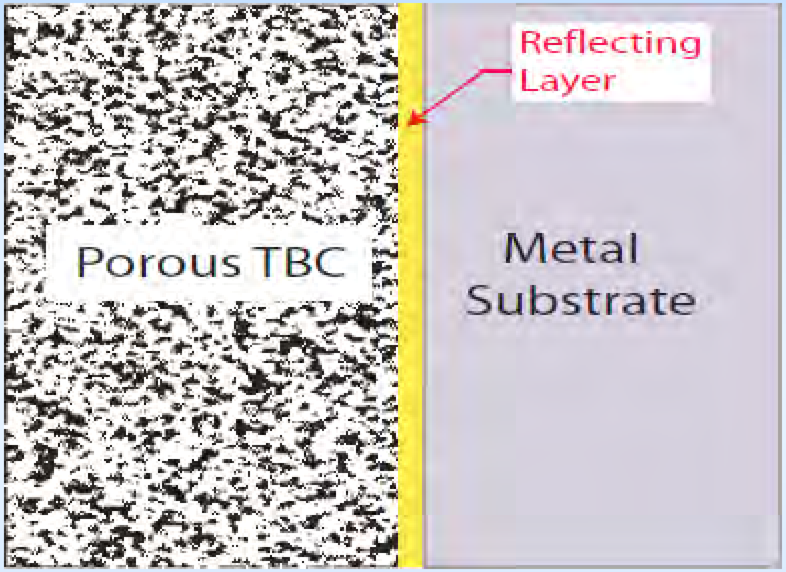

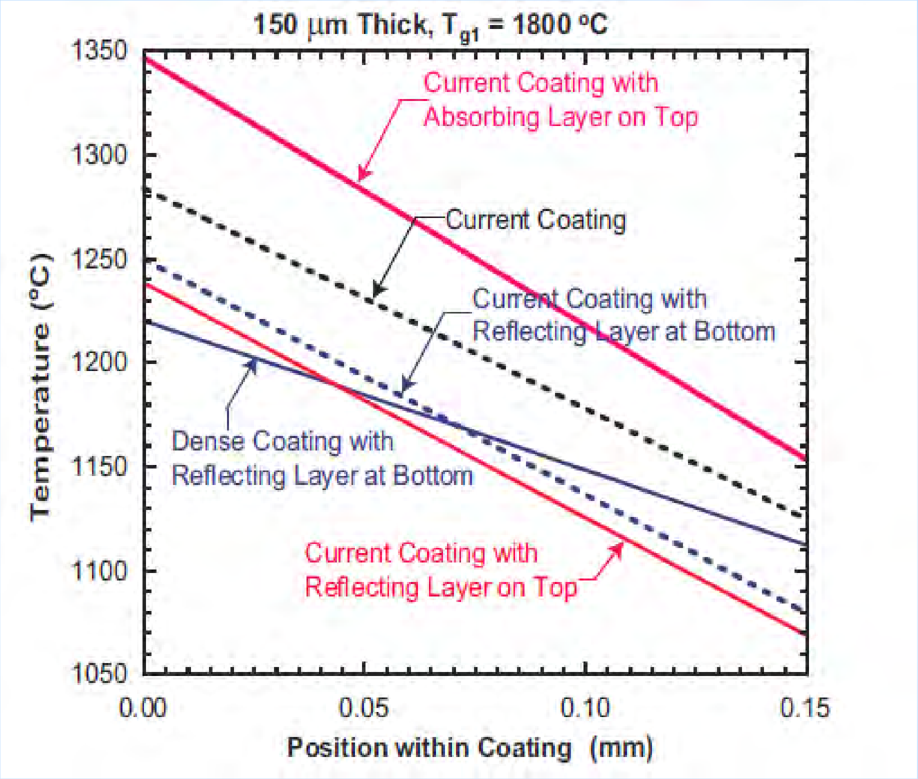

Liguo Chen, Phd Thesis

Basis of Optical Probing of a TBC

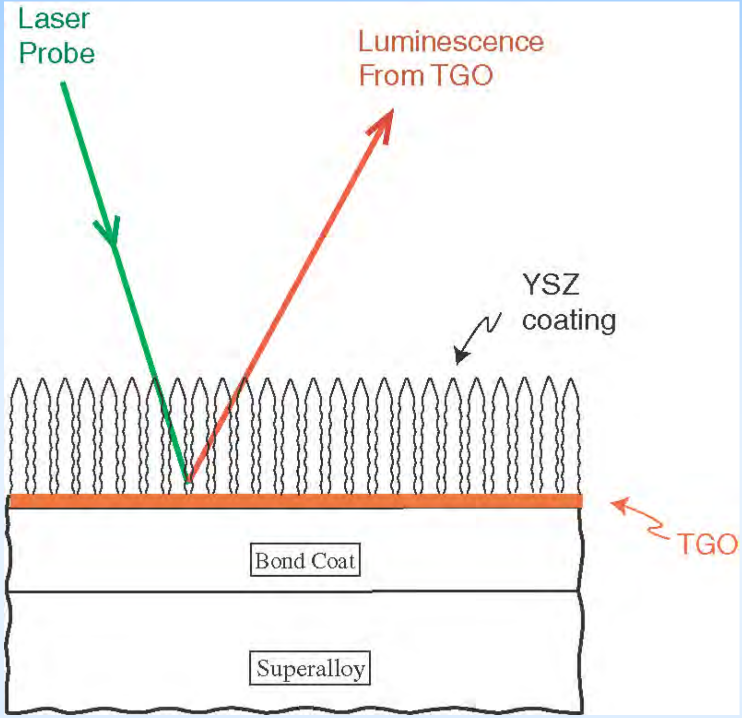

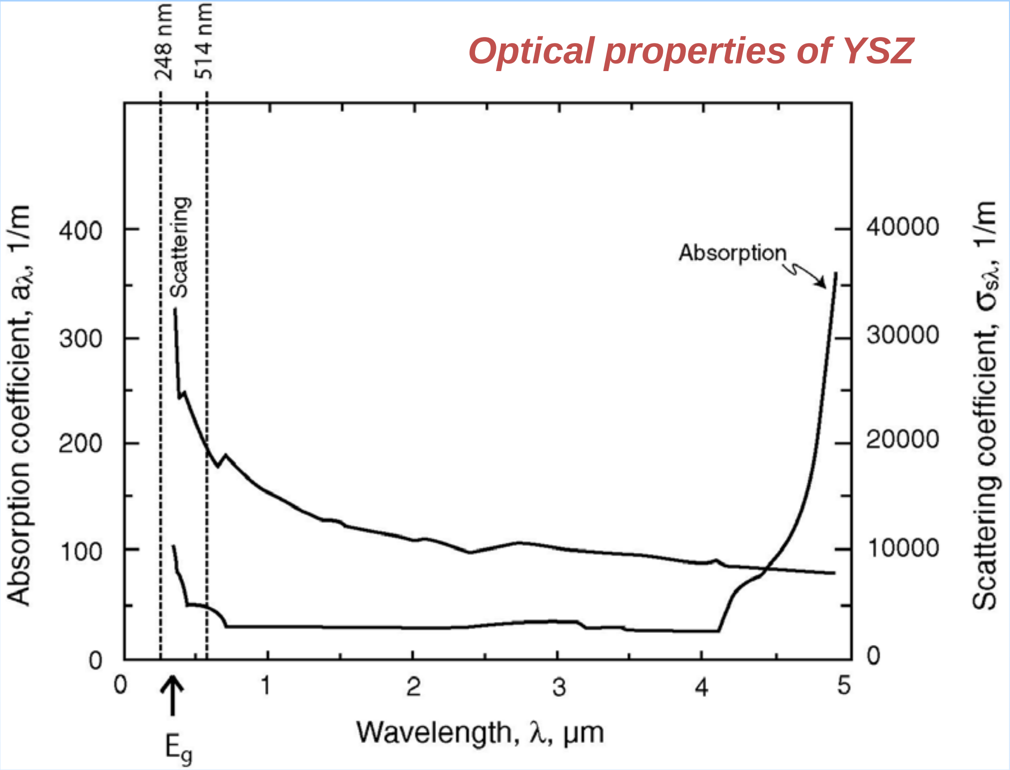

TBCs are optically turbid media – highly scattering but are translucent
Hence some light can penetrate through to the TGO underneath the TBC

Luminescence Based Temperature and Damage Sensor

Non-contact method

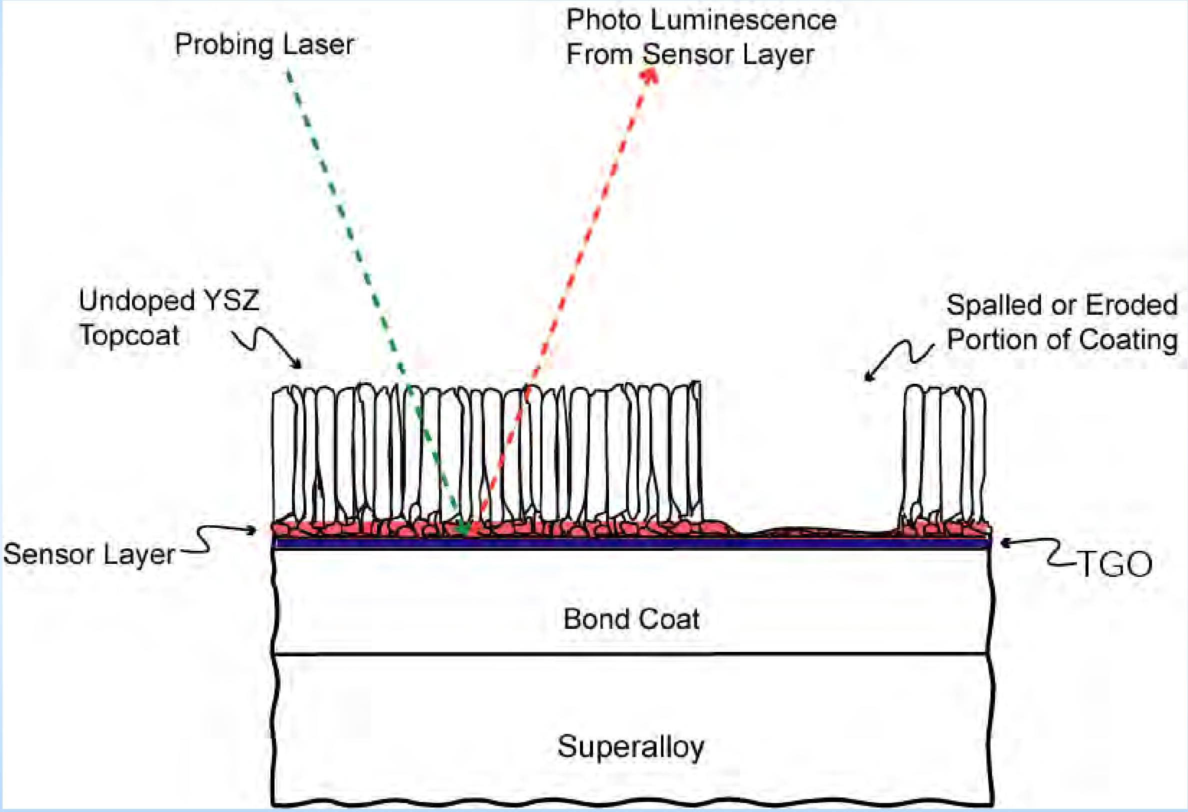

- Luminescent ions can be incorporated into crystal structure of the coating material to act as sensors
- Luminescence lifetime is known to be temperature sensitive
- Because of translucency of TBC materials, visible lasers and luminescence can be used to measure temperatures of sensors buried in a coating
- Multiple sensor layers can be applied to measure the temperature at any depth

Example: Eu Doped TBC Sensor Layer

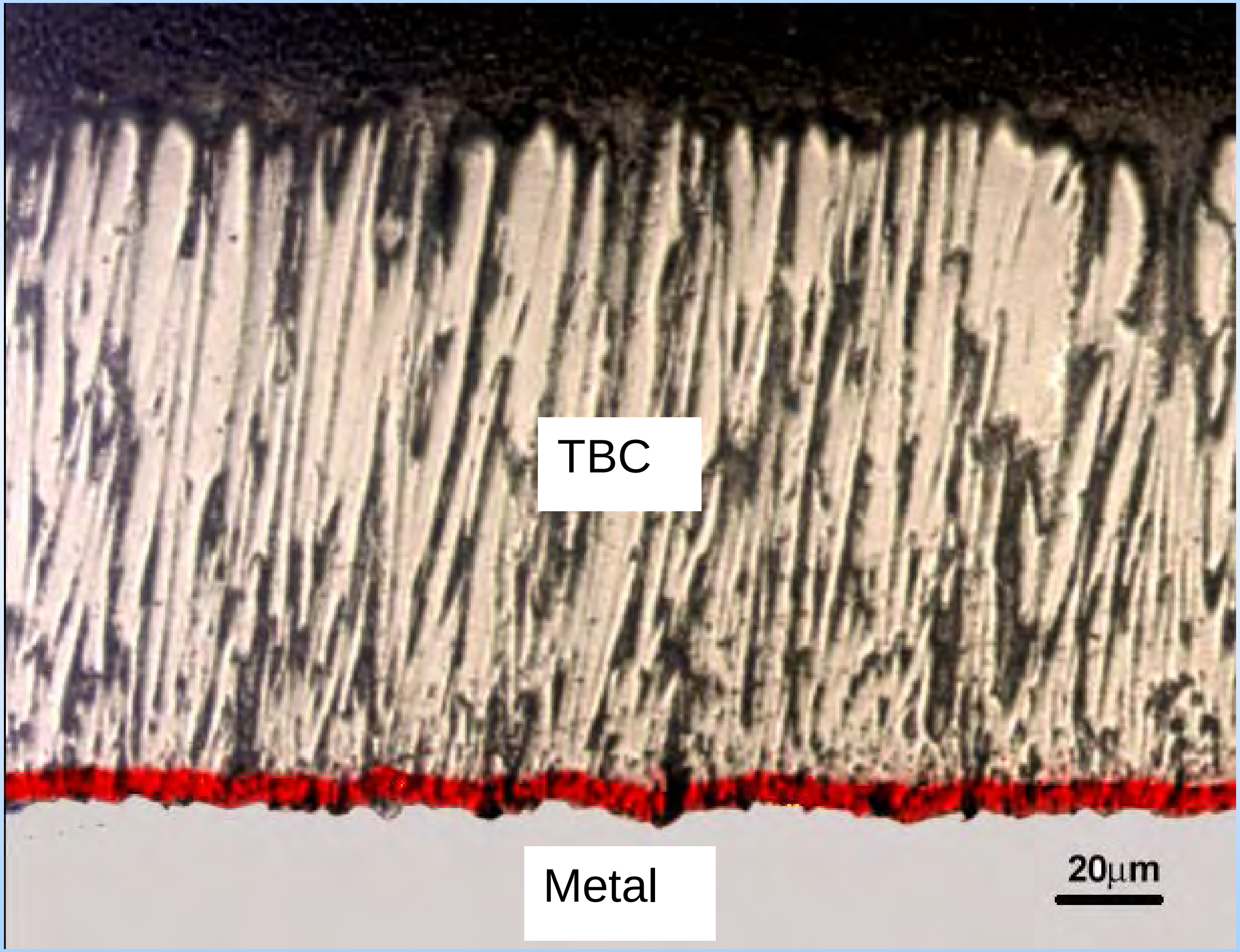

Superimposition of white light and UV luminescence images

D. R. Clarke, Harvard University, Jan 2015

Temperature Sensing Using Luminescence Lifetimes

10 micron Eu-doped sensor layer in a EB-PVD YSZ coating

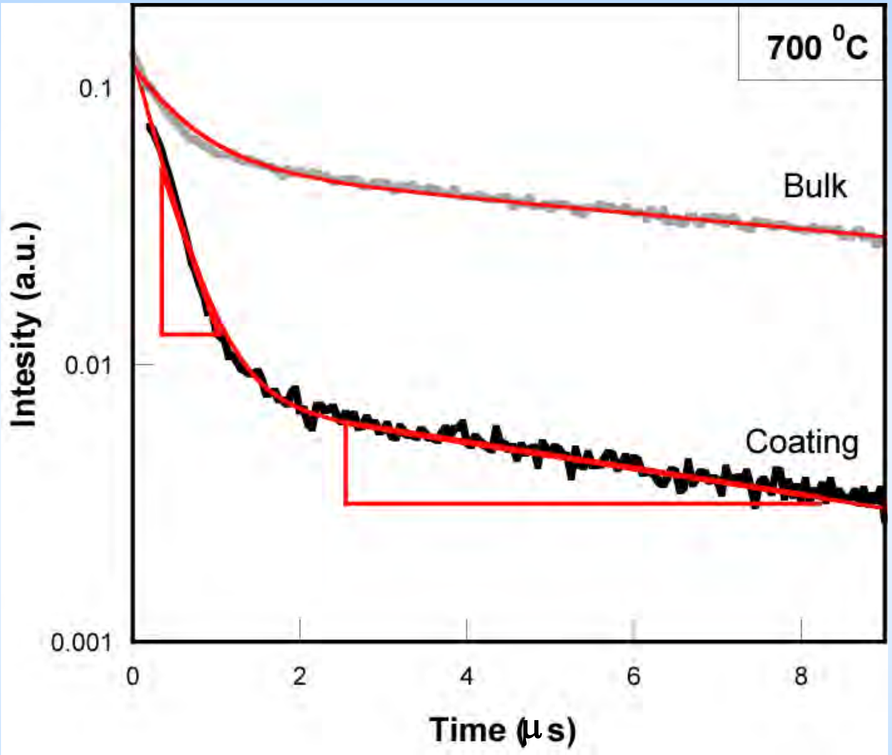

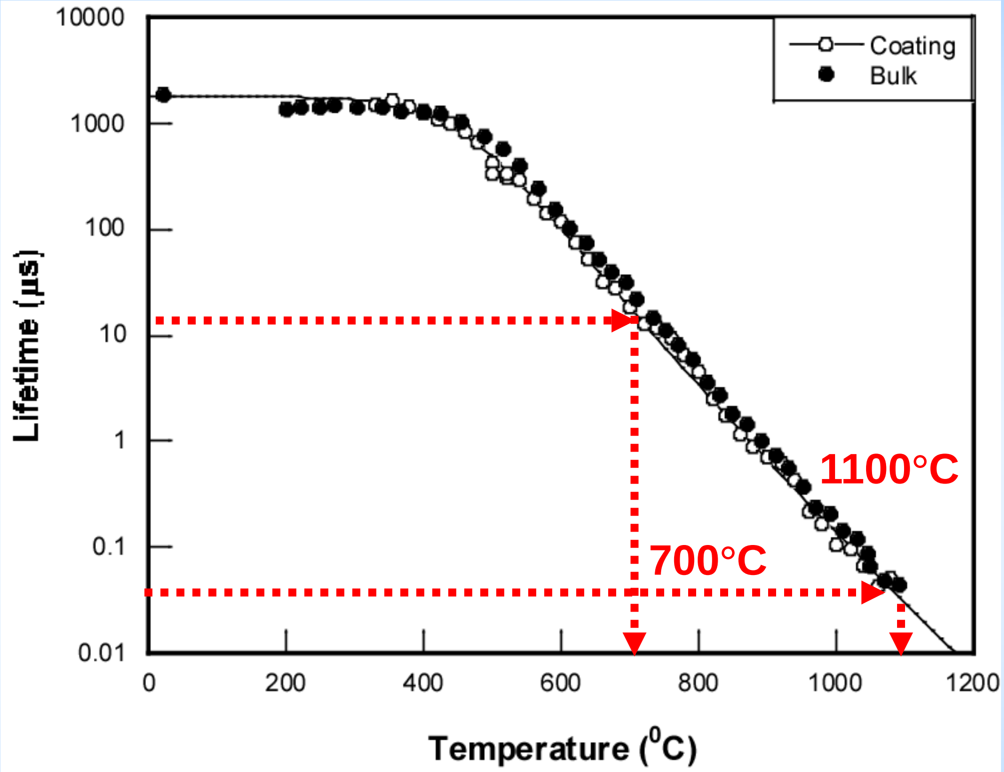

Calibration of luminescence lifetime provides basis for temperature measurements on engine components

TBC Interface Temperature in a Thermal Gradient

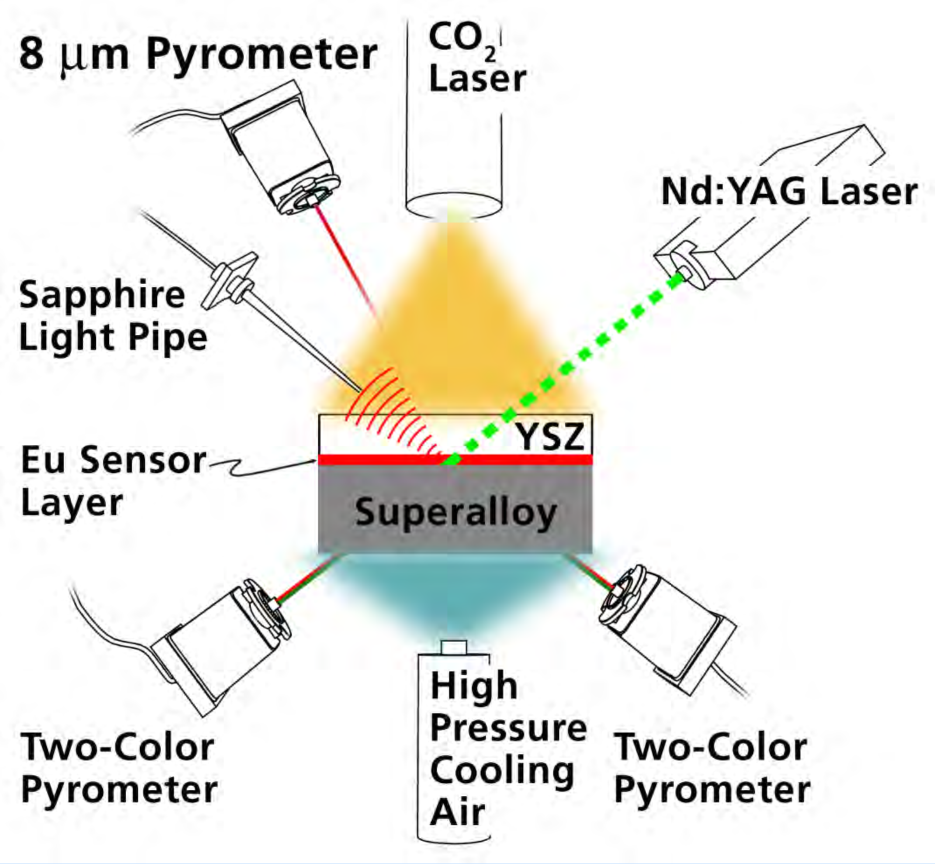

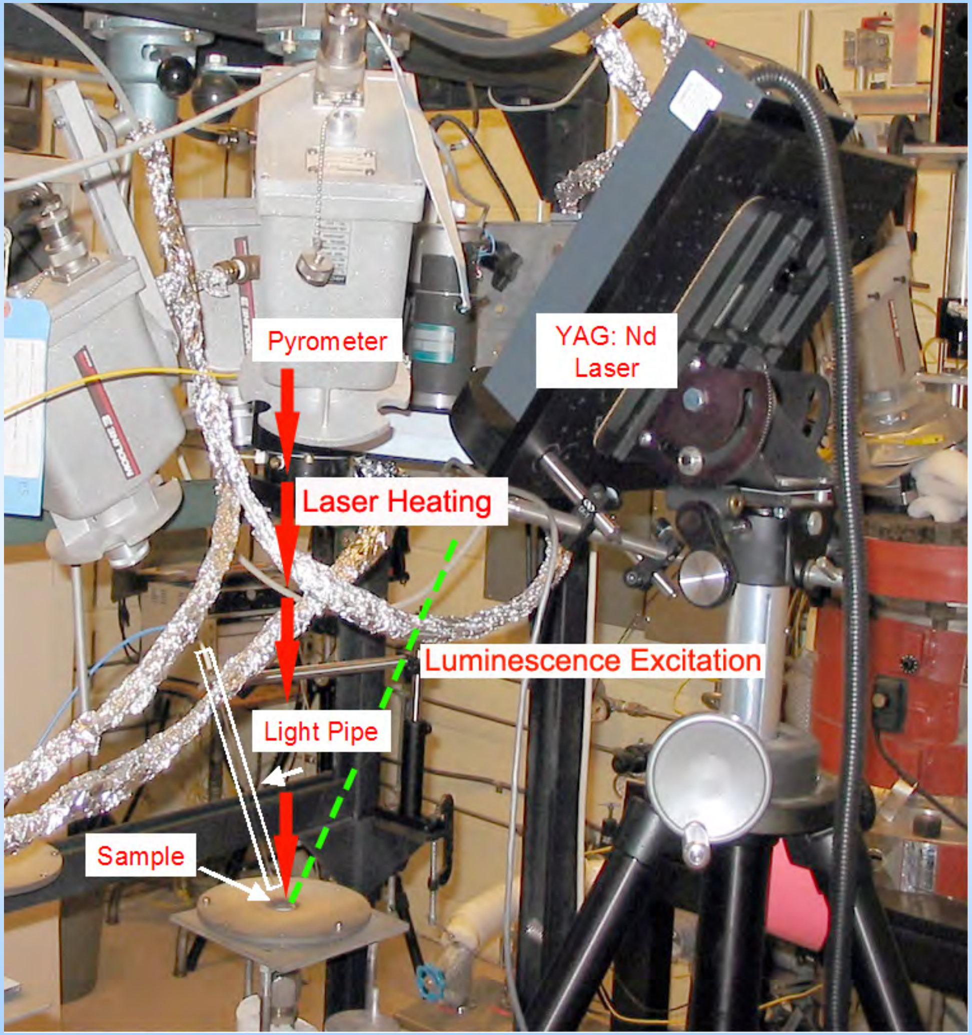

with D. Zhu and J. Eldridge, NASA Glenn. Surf Coat Tech Vol 201 (2006)

TBC Interface Temperature in a Thermal Gradient

TBC thickness: 146 μm

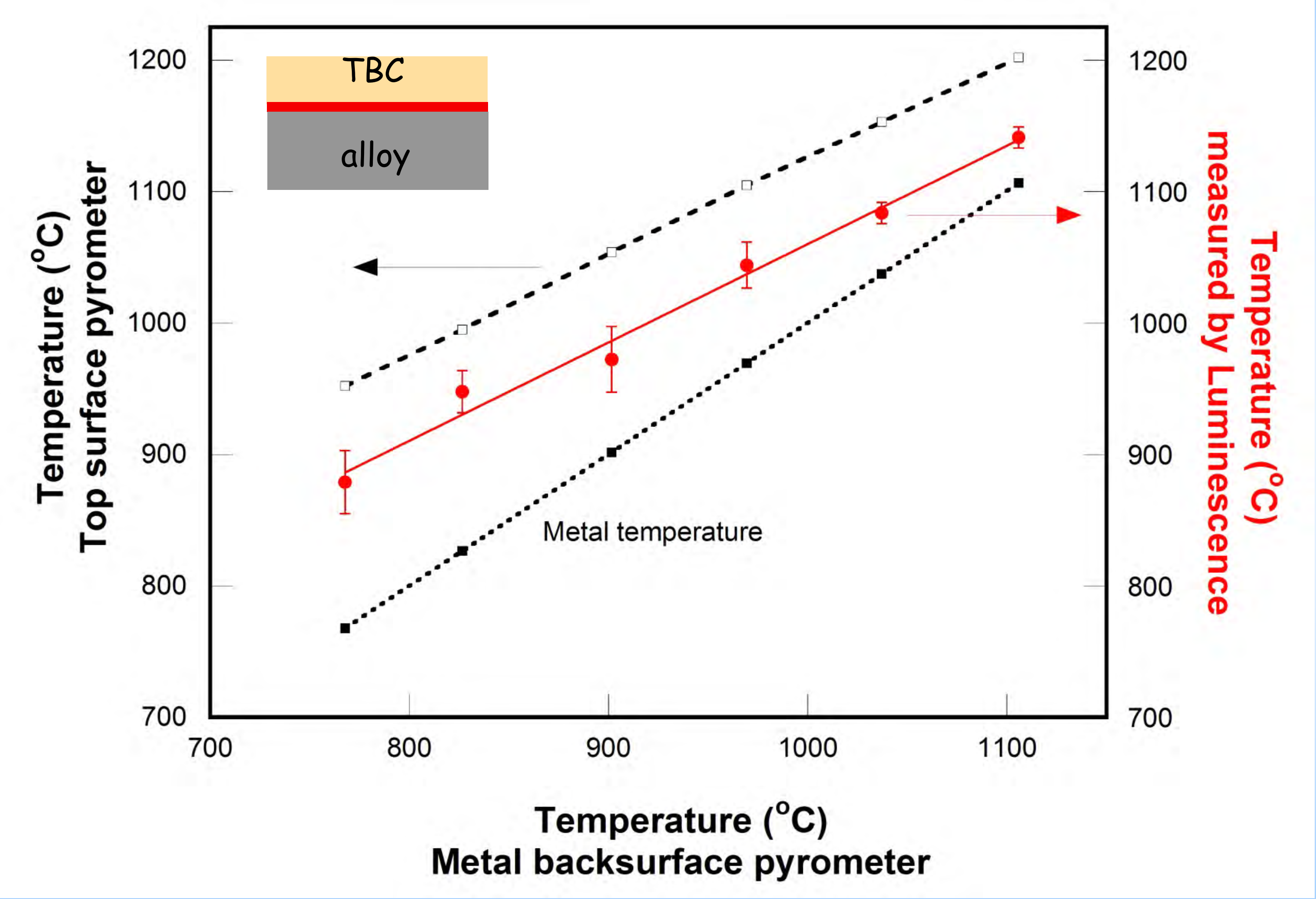

Effect of Thermal Cycling on Coating Life

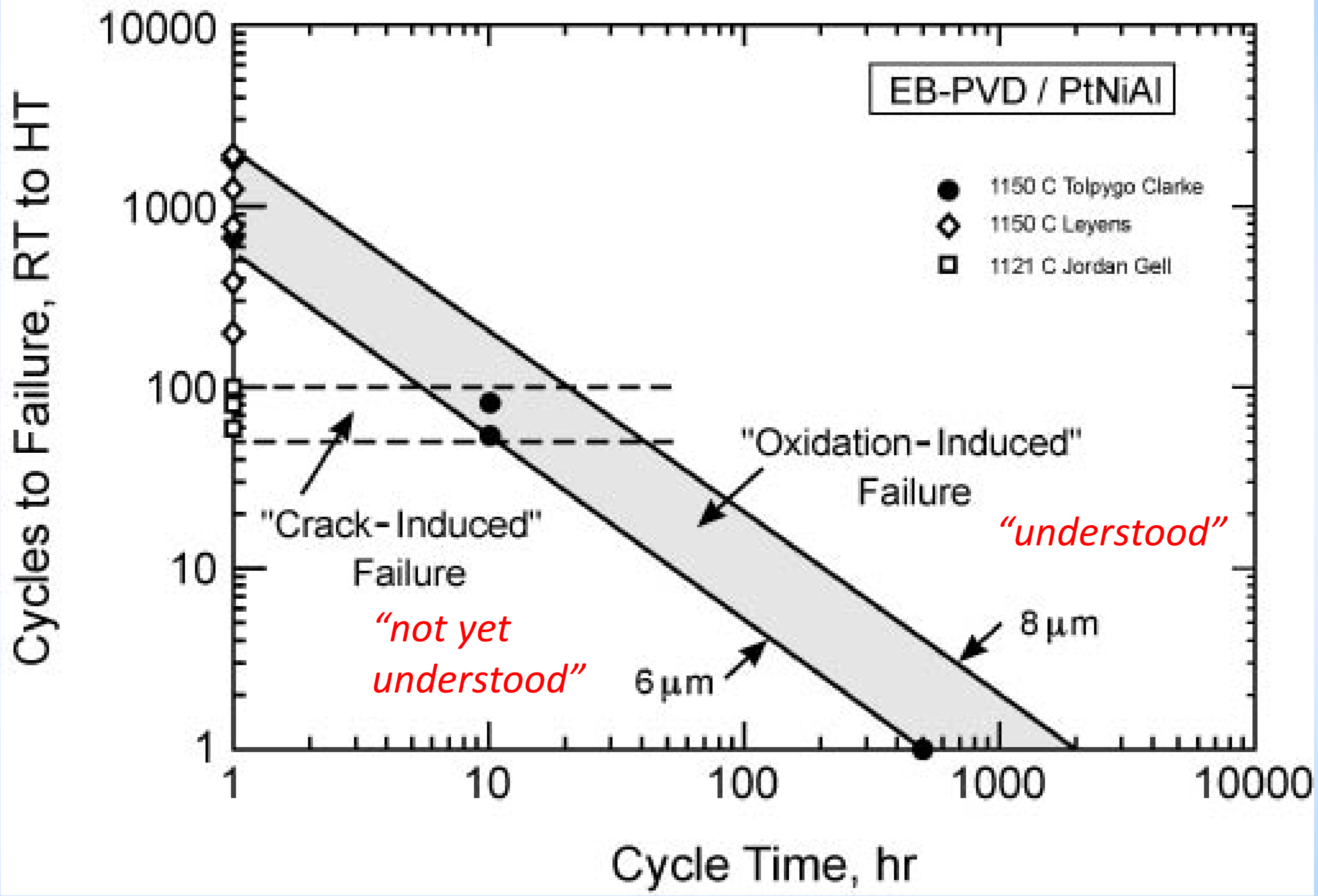

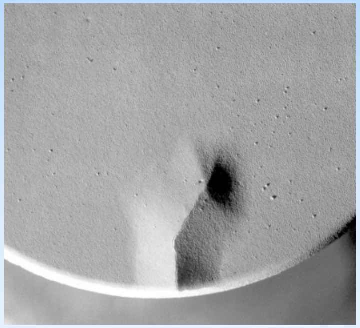

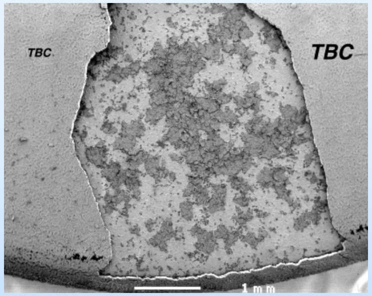

SWRI report

Thermal Cycling Instability

Life of TBC is often limited by morphological instability ("rumpling") of the metal bond coat on thermal cycling causing incompatibilities with TBC. More stable alloys needed

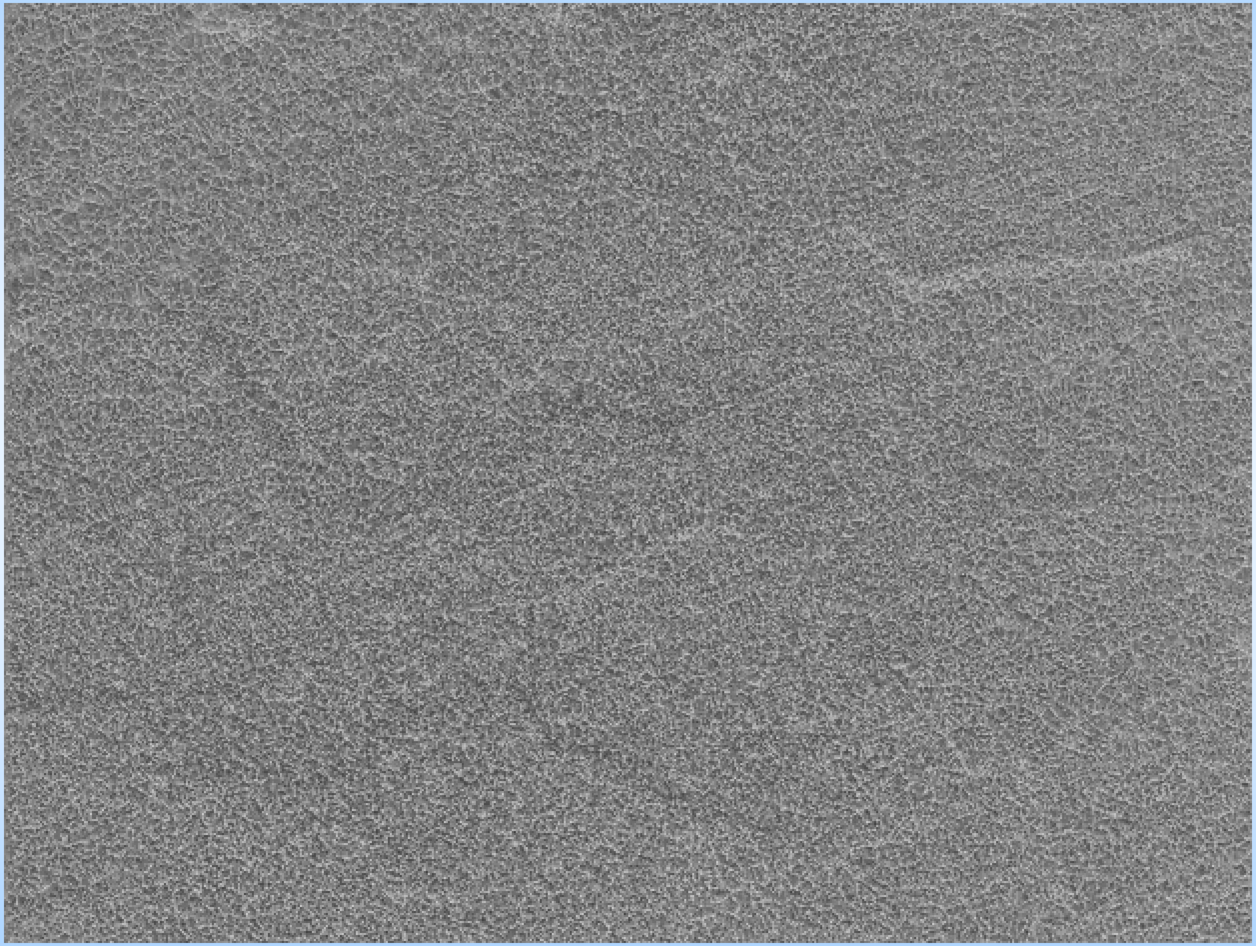

Coating surface on thermal cycling.

0-300 cycles to 1150^{o}C in air. ~ 400 micron field of view

D. R. Clarke, Harvard University, Jan 2015

TBC Interface after 100 One-hour Cycles to 1150^{o}C

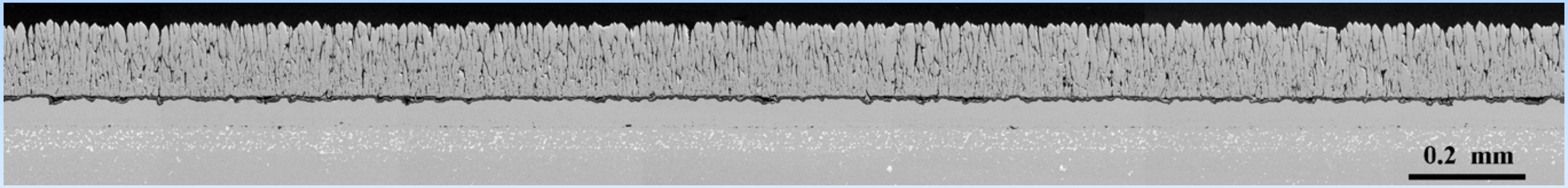

Low magnification

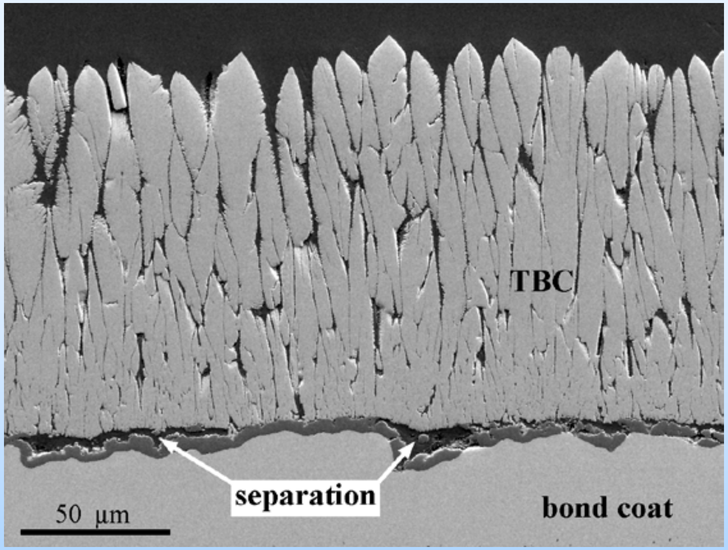

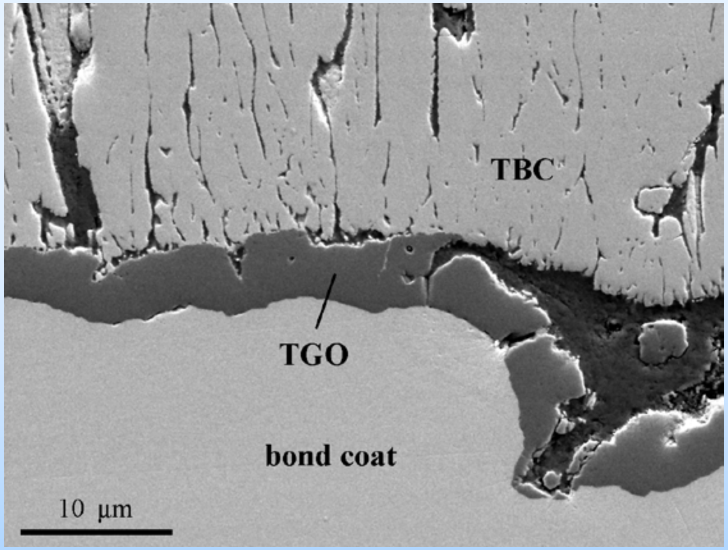

Evolution of Interface Separation Leading to Failure

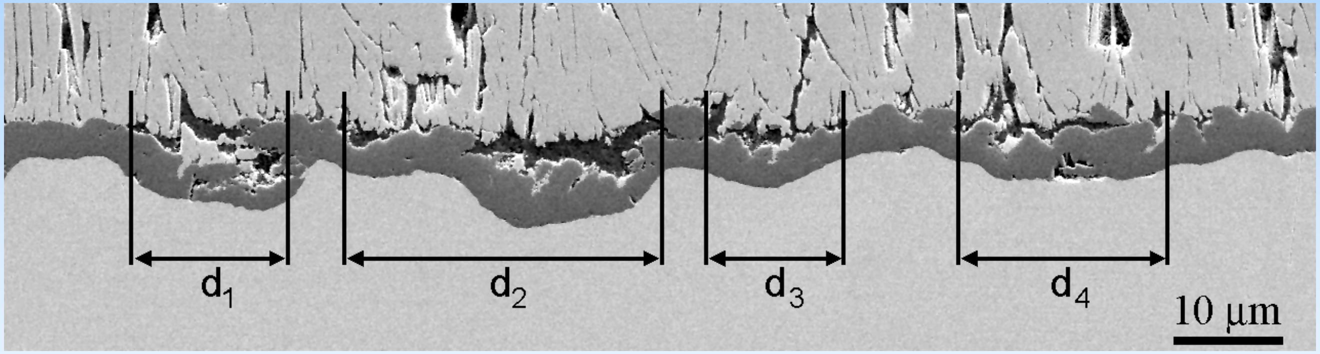

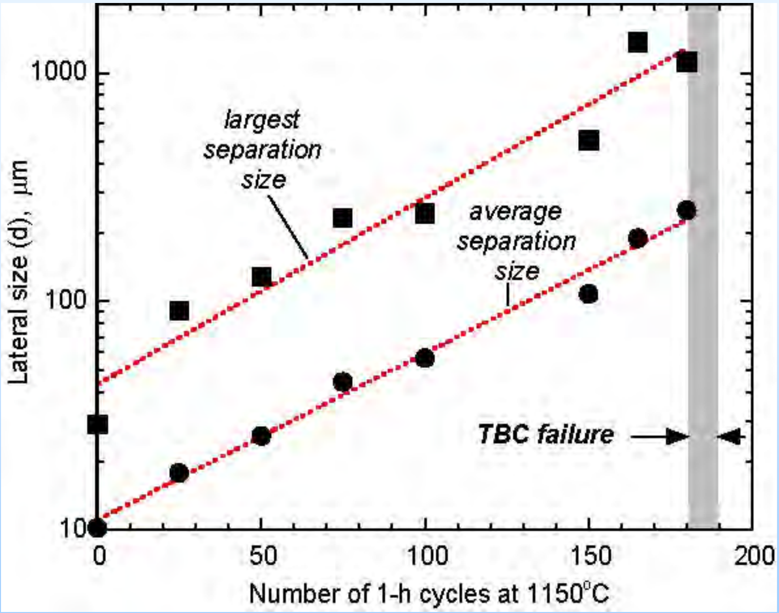

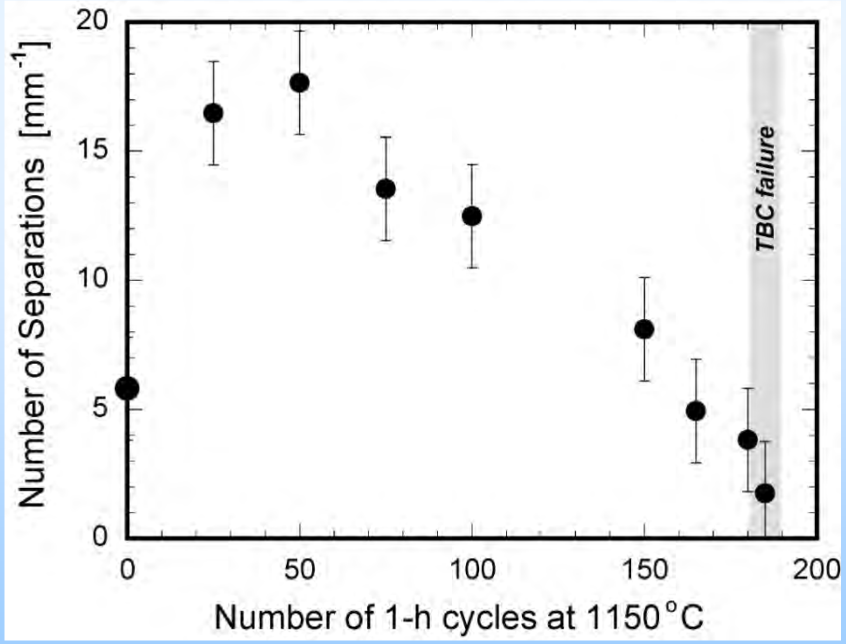

Tolpygo, Murphy, Clarke

R-line Luminescence and Piezospectroscopy

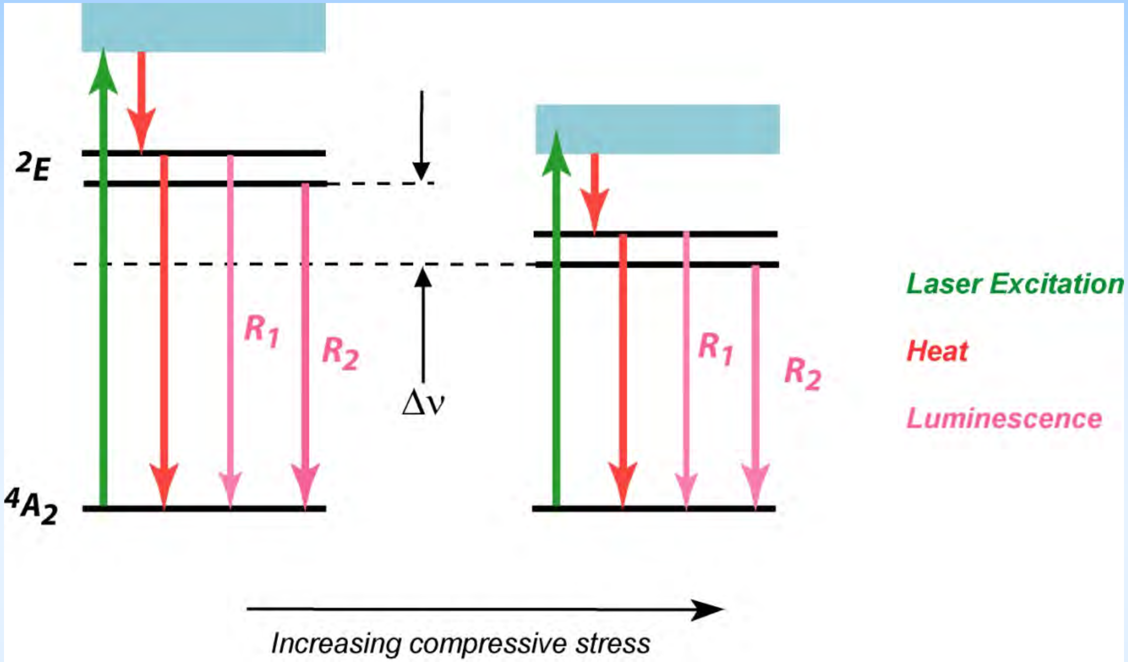

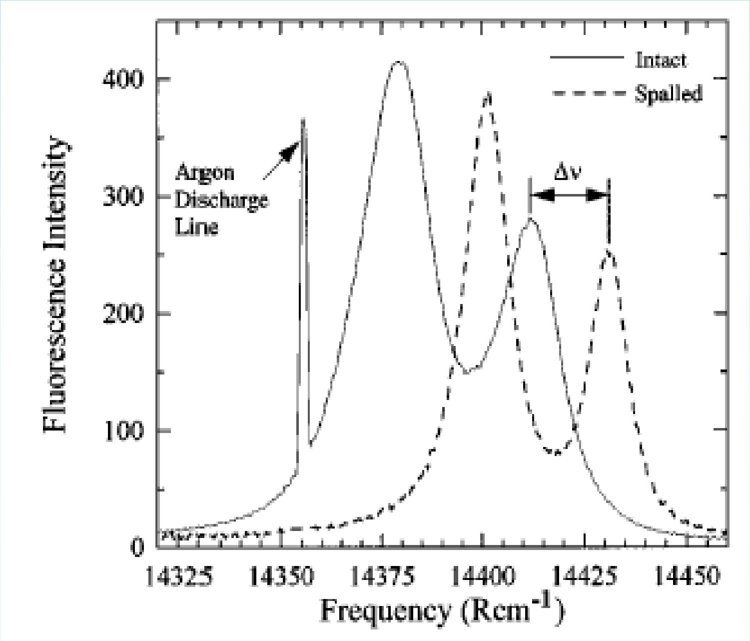

Key concepts:

- *All alumina contains small (ppm) concentrations of Cr^{3+} in solid solution*
- *Each Cr^{3+} ion emits photons with an energy dependent on its own local strain environment*
- *Frequency shift proportional to mean stress in a polycrystalline alumina*

$$\Delta \nu_{R2} = 7.62\,\sigma_m$$

Basis of Optical Probing of a TBC

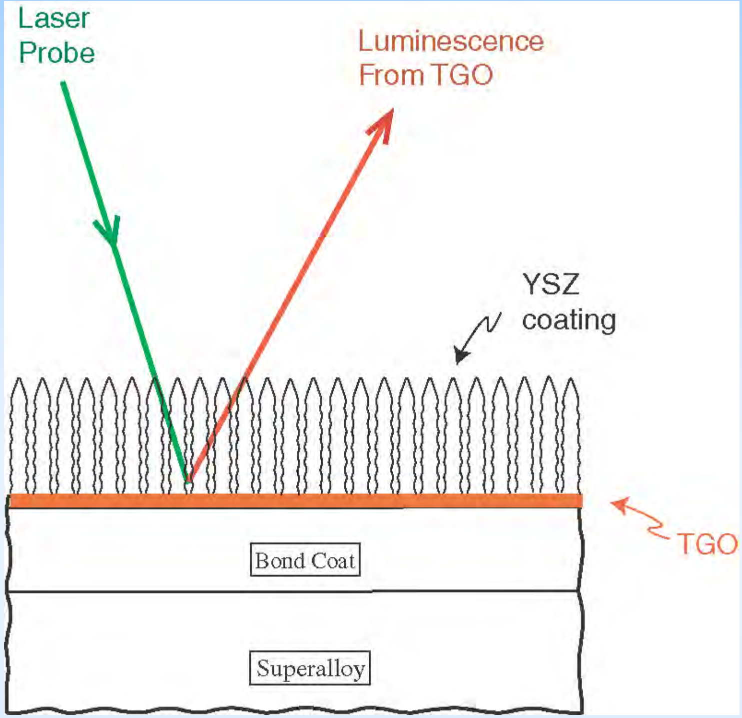

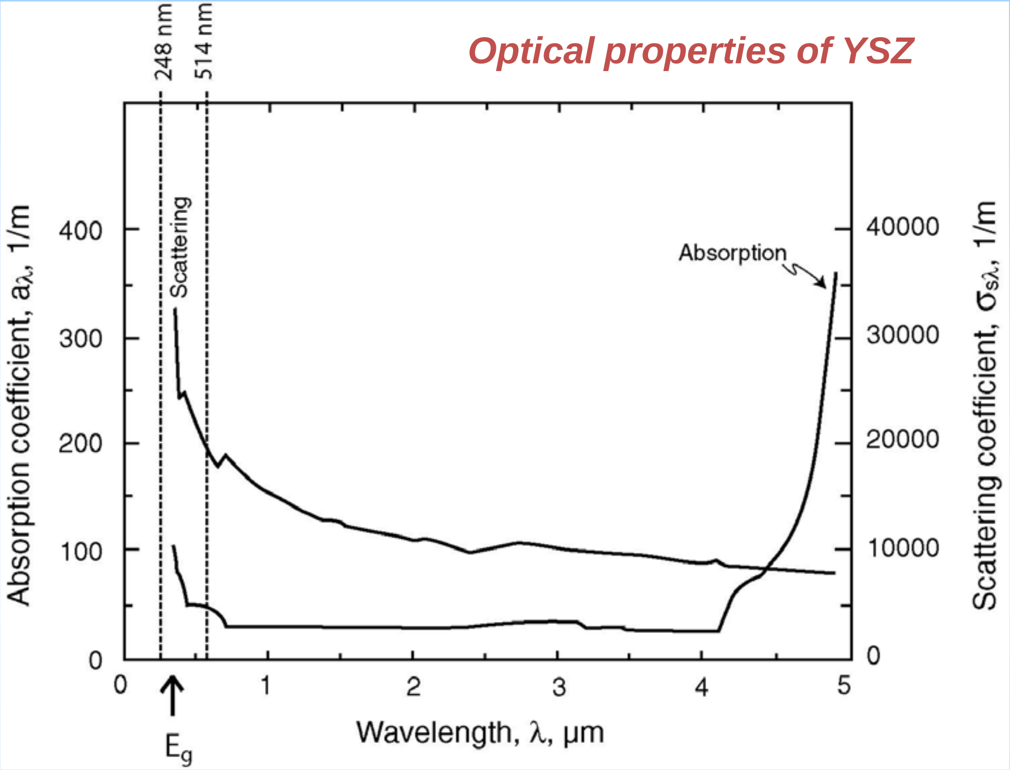

TBCs are optically turbid media – highly scattering but translucent
Hence some light can penetrate through to the TGO underneath the TBC

Multi-spectral Luminescence Imaging to Reveal Stress Variations

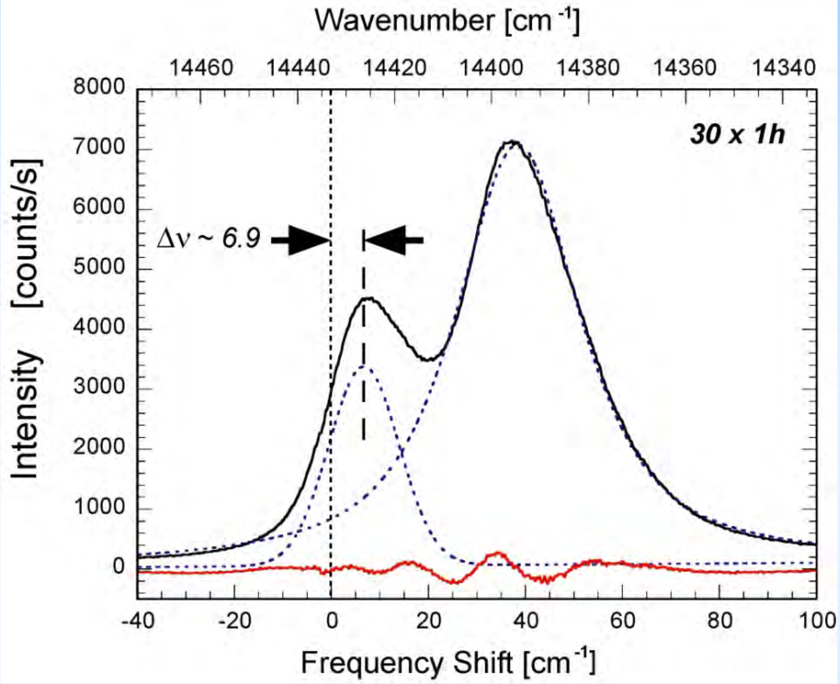

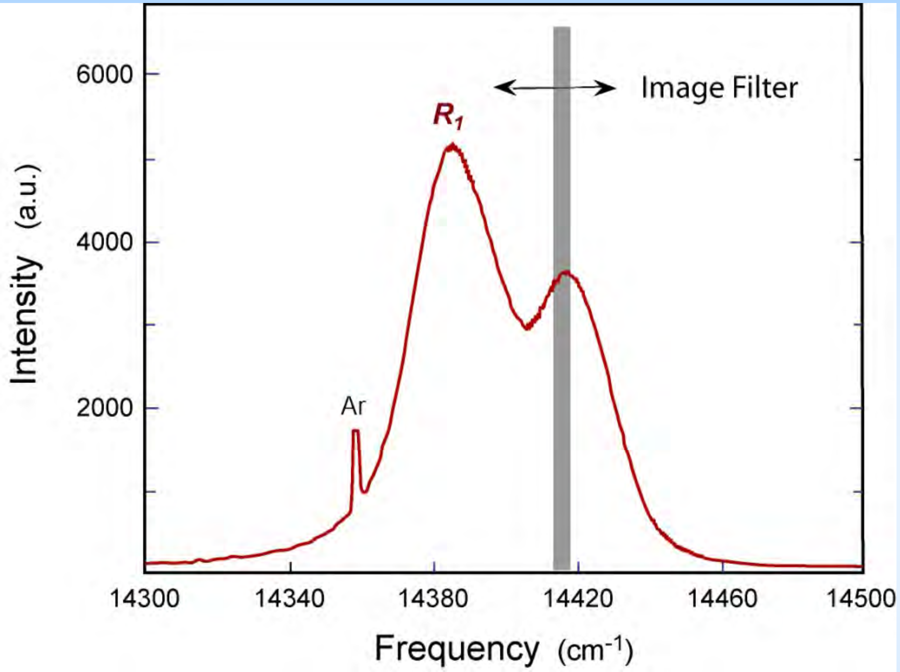

- Illuminate coating with uniform laser beam, 514.3 nm
- Collect R-line luminescence on a CCD through a tunable Fabry-Perot filter
- Tune filter through the luminescence frequency band recording an image at each frequency step
- Invert spectral images to determine R1 shift and hence stress at each image pixel
- Map stress distribution over coating

1.15 – 1.20 GPa

WA12

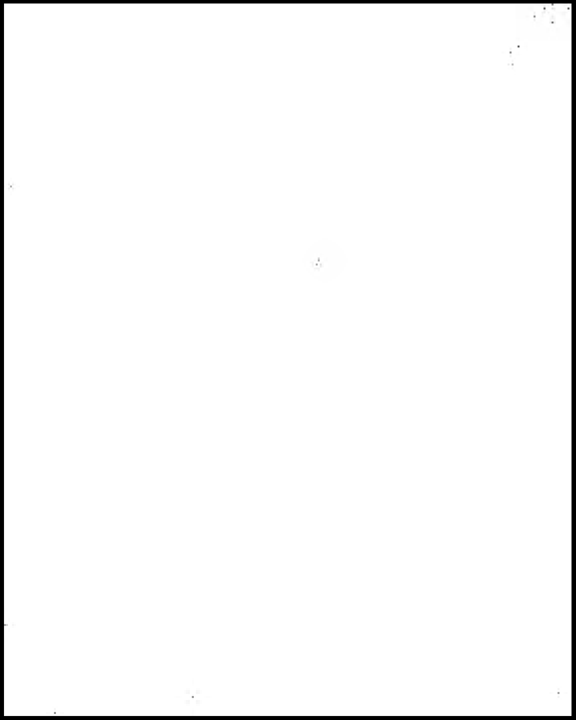

WA15

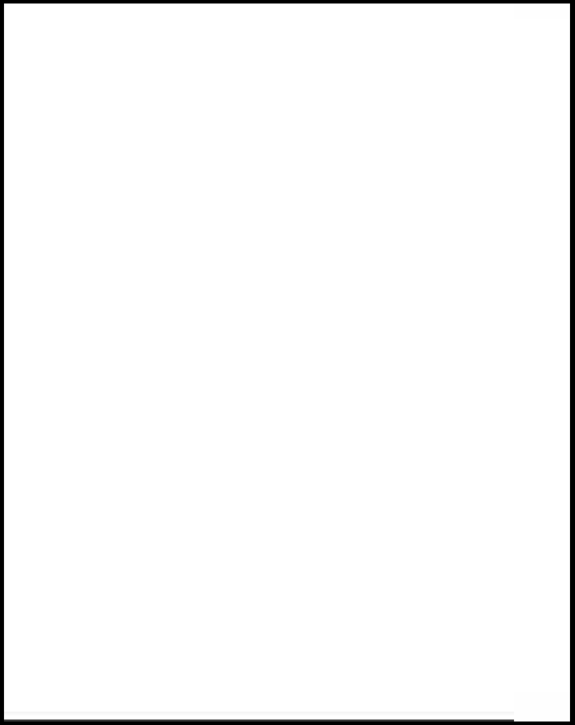

1.10 – 1.15 GPa

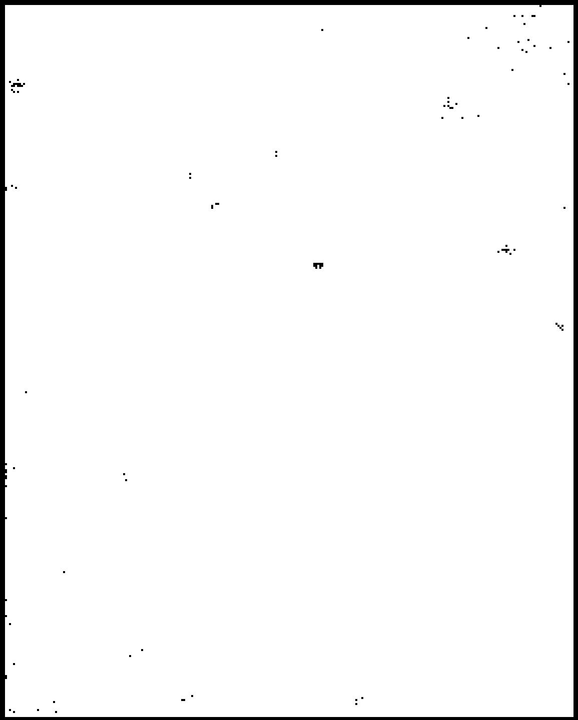

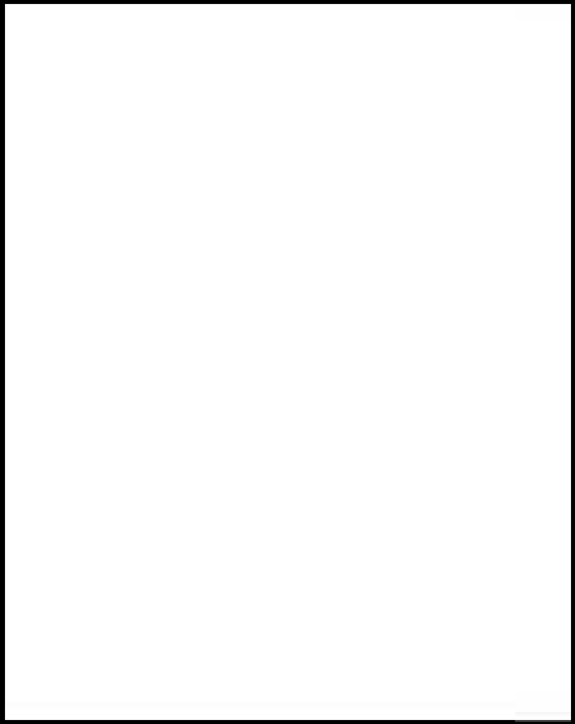

1.05 – 1.10 GPa

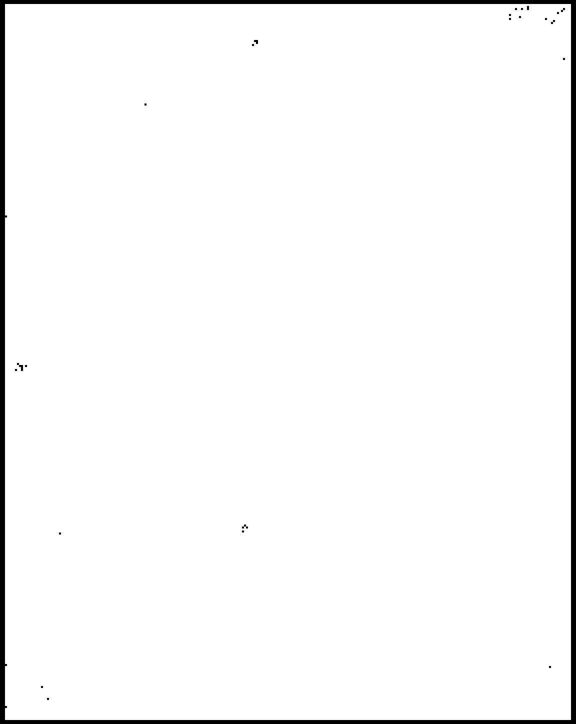

1.00 – 1.05 GPa

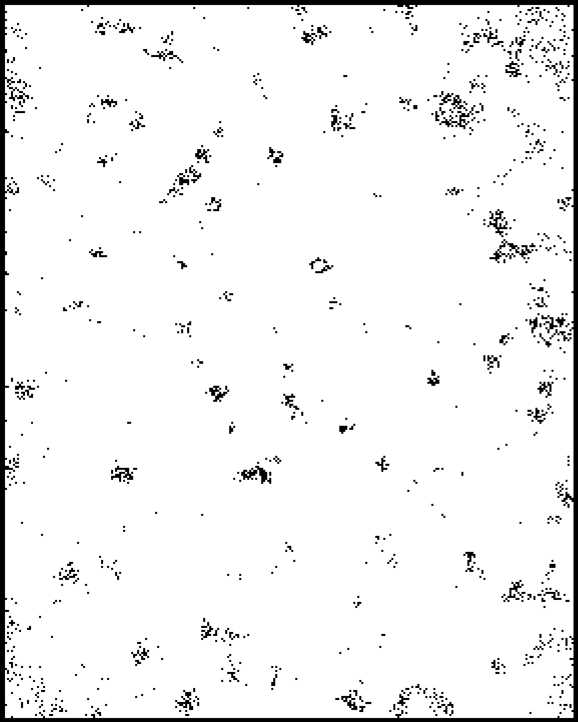

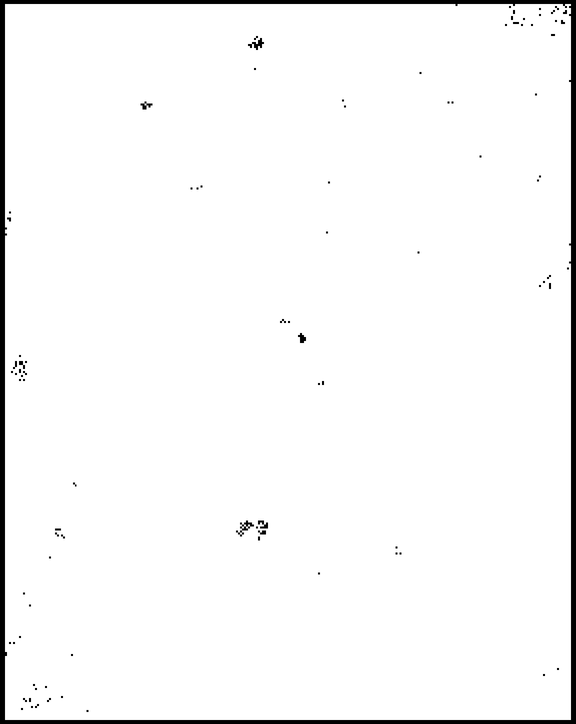

0.95 – 1.00 GPa

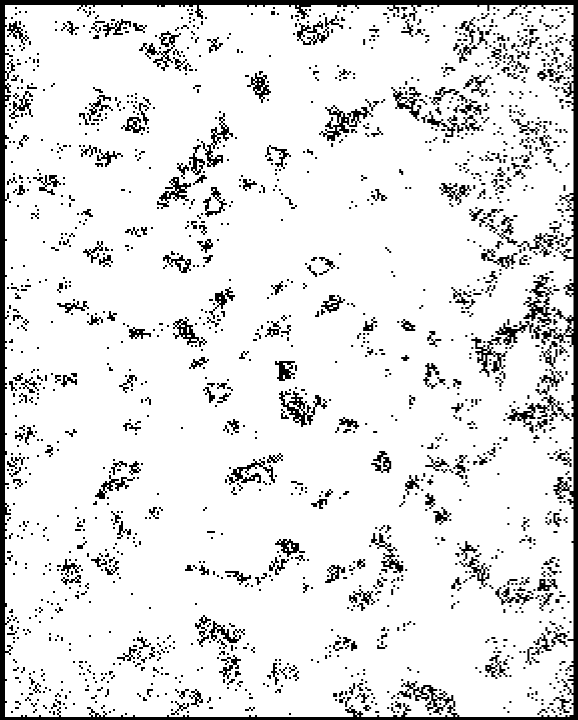

0.90 – 0.95 GPa

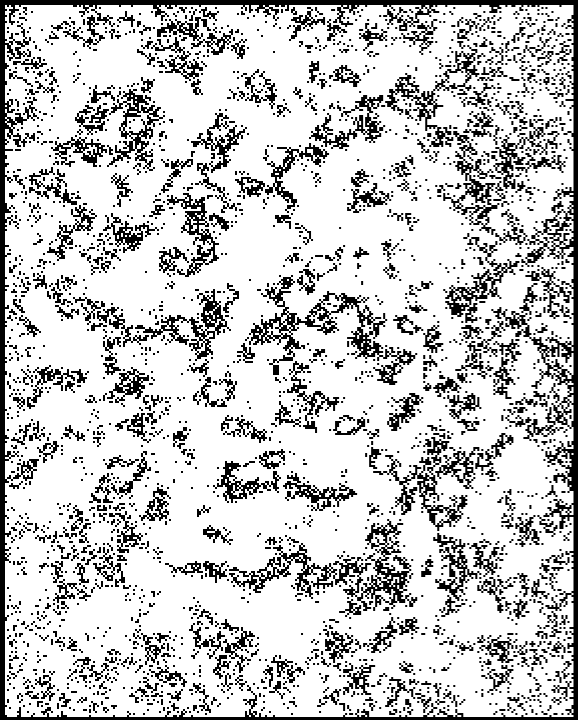

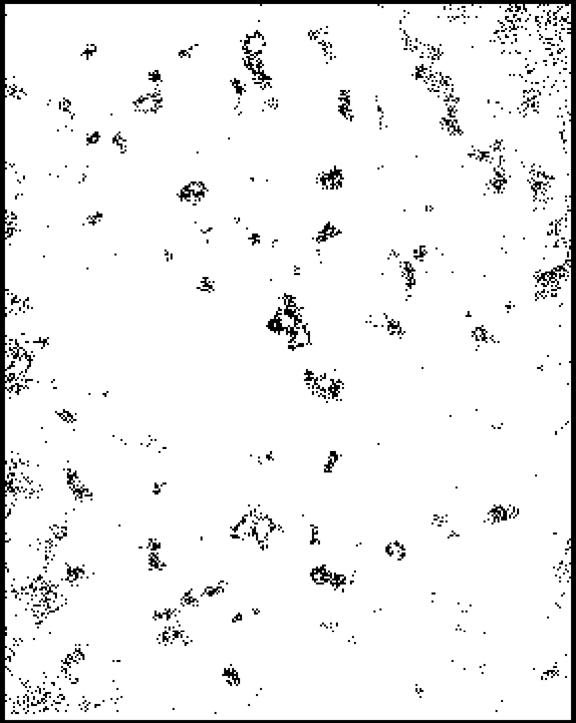

0.85 – 0.90 GPa

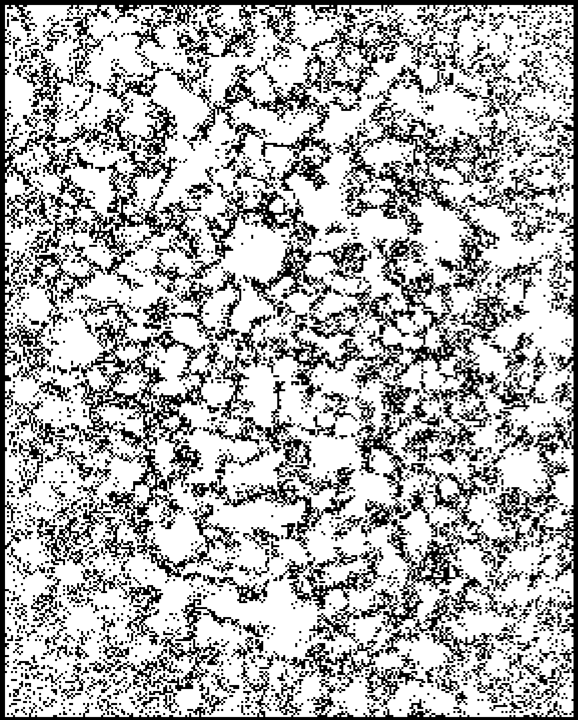

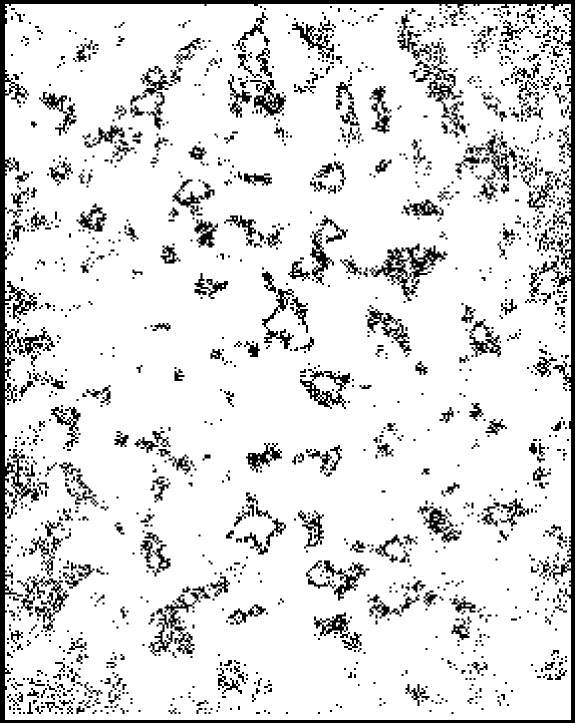

0.80 – 0.85 GPa

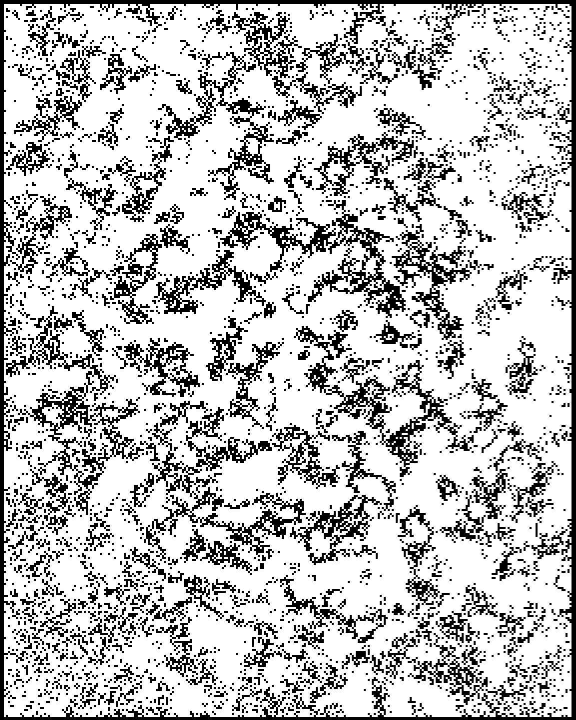

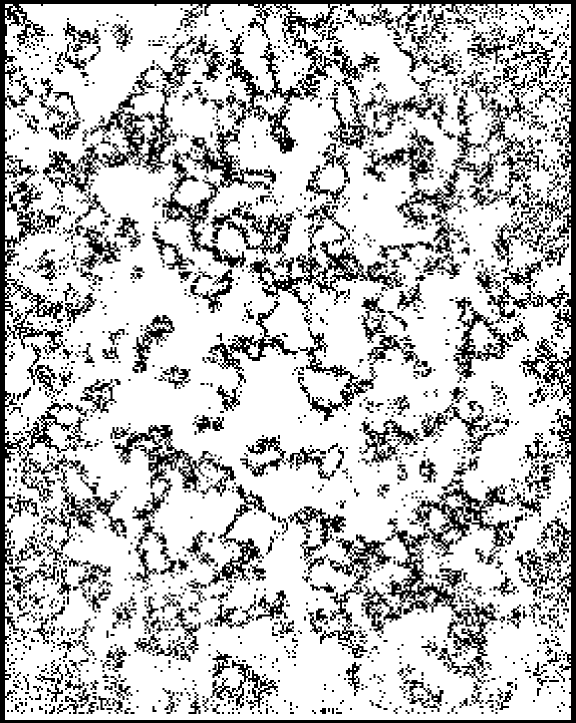

0.75 – 0.80 GPa

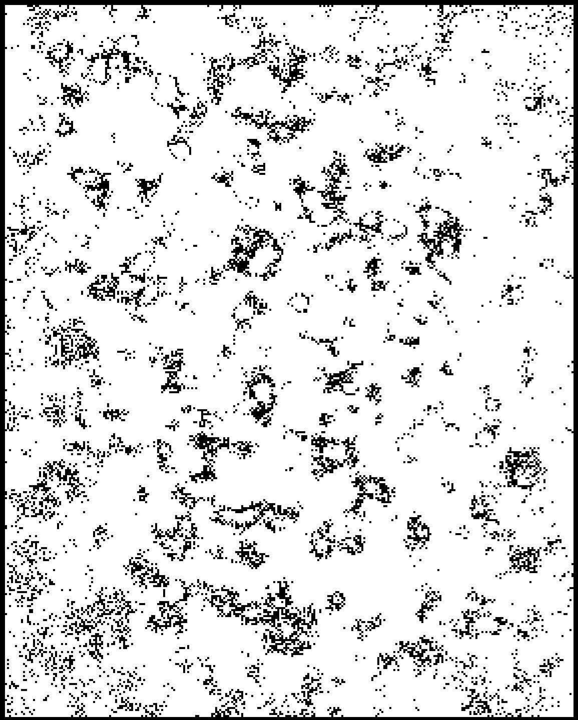

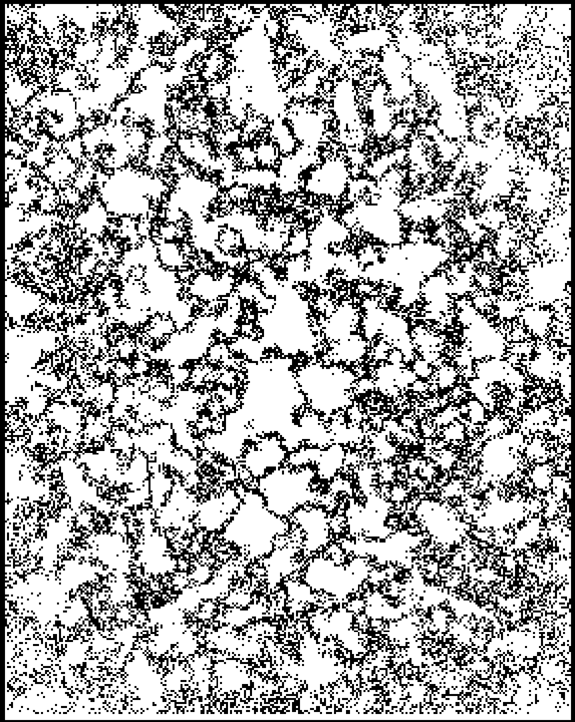

0.70 – 0.75 GPa

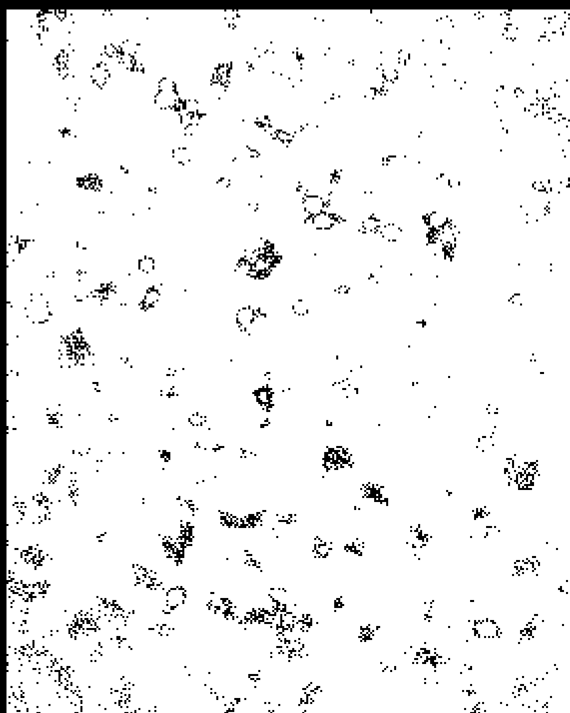

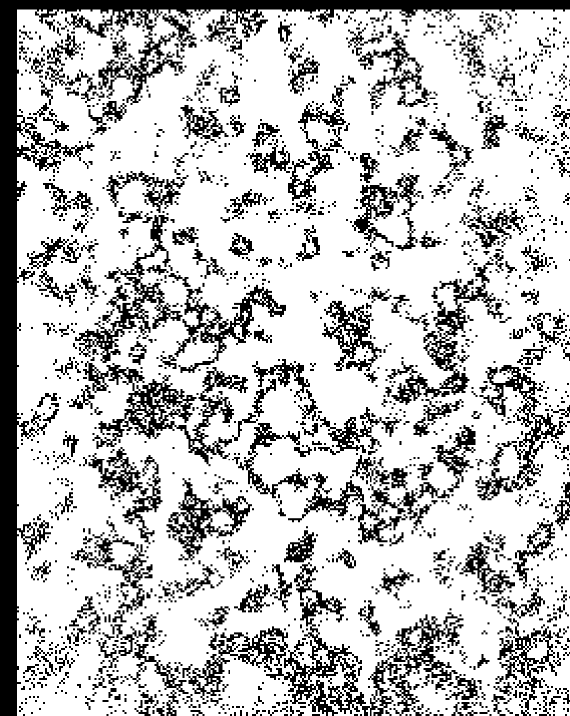

0.65 – 0.70 GPa

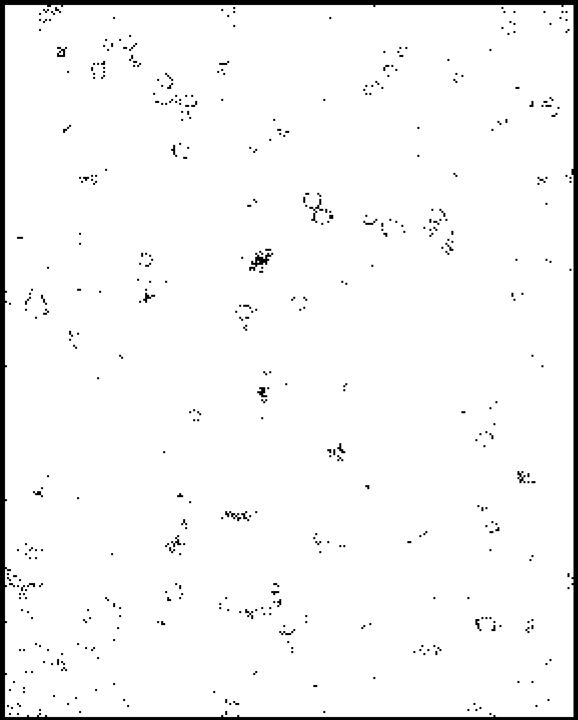

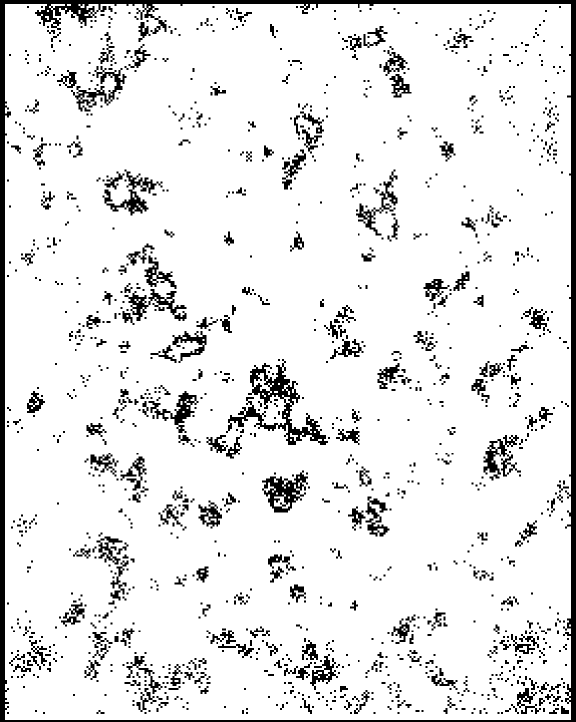

0.60 – 0.65 GPa

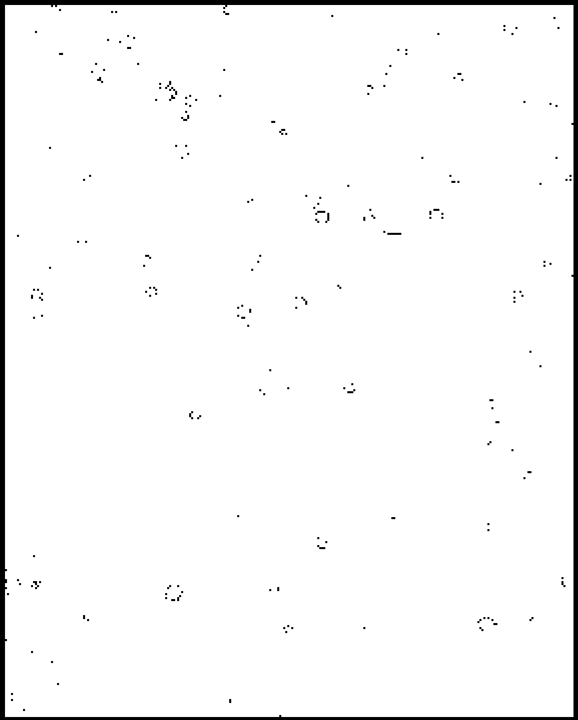

0.55 – 0.60 GPa

0.50 – 0.55 GPa

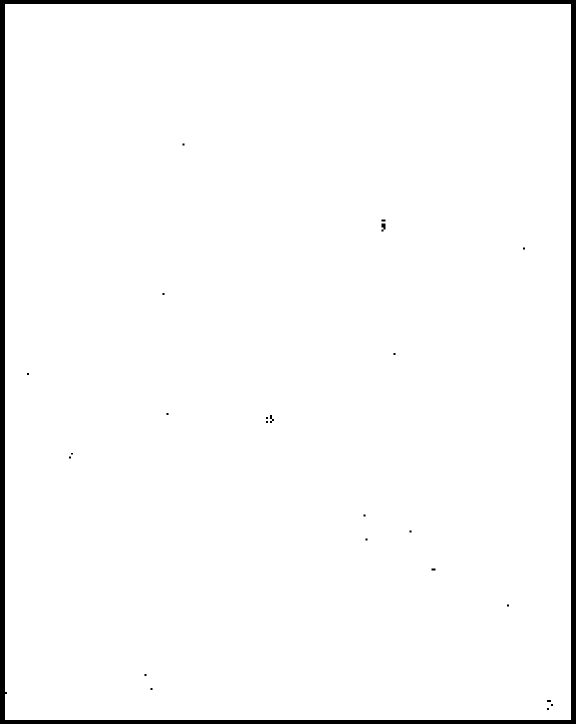

Evolution of Interface Damage with Thermal Cycling

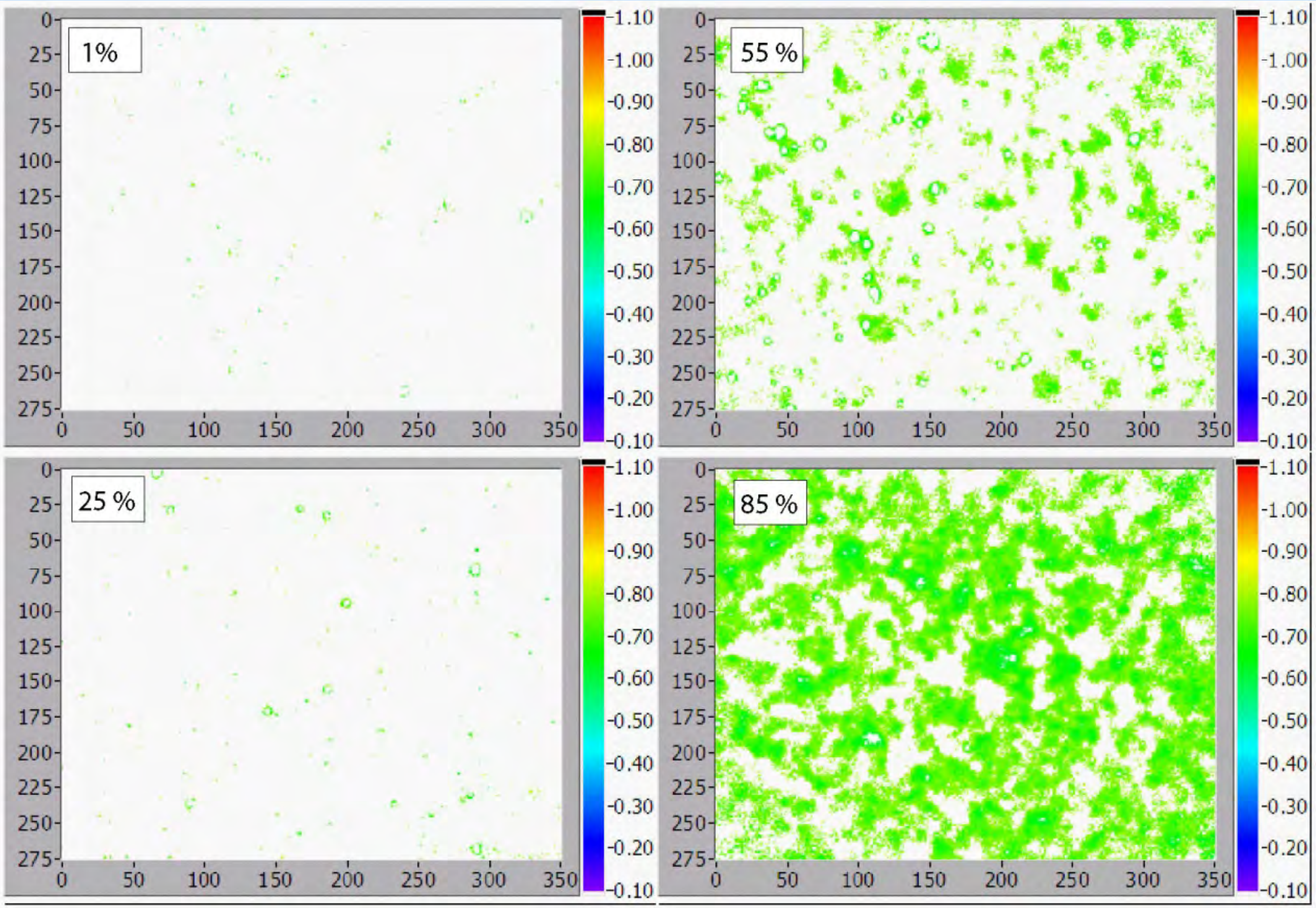

Percolation of separated regions !

Green areas correspond to areas where the mean stress below 0.7 GPa

D. R. Clarke, Harvard University, Jan 2015

Vibrational Damping Due to Oxygen Hopping

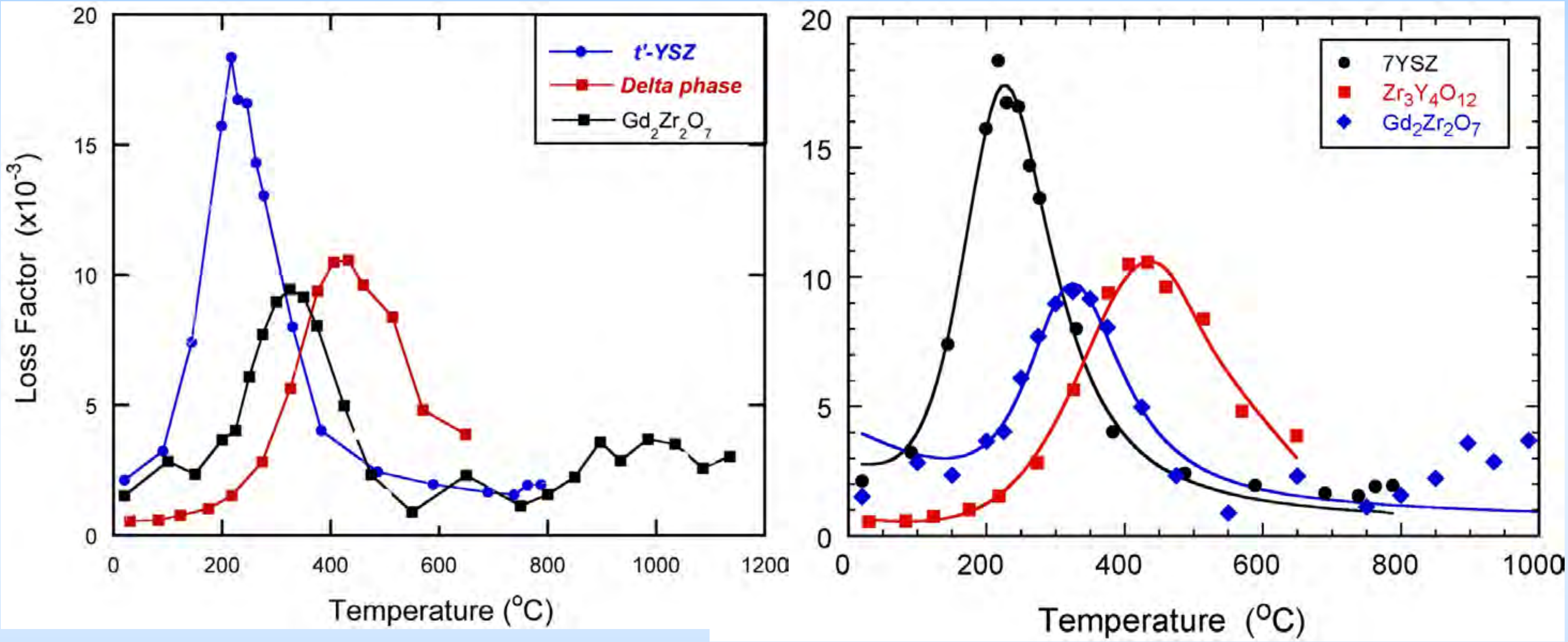

Defect Rearrangement Model (Wachman) predicts that damping peak occurs at:

$$T_p = \frac{E_i}{k_B \ln \omega \tau}$$

Activation energy for hopping

The Next Materials Frontier: Ceramic Matrix Composites

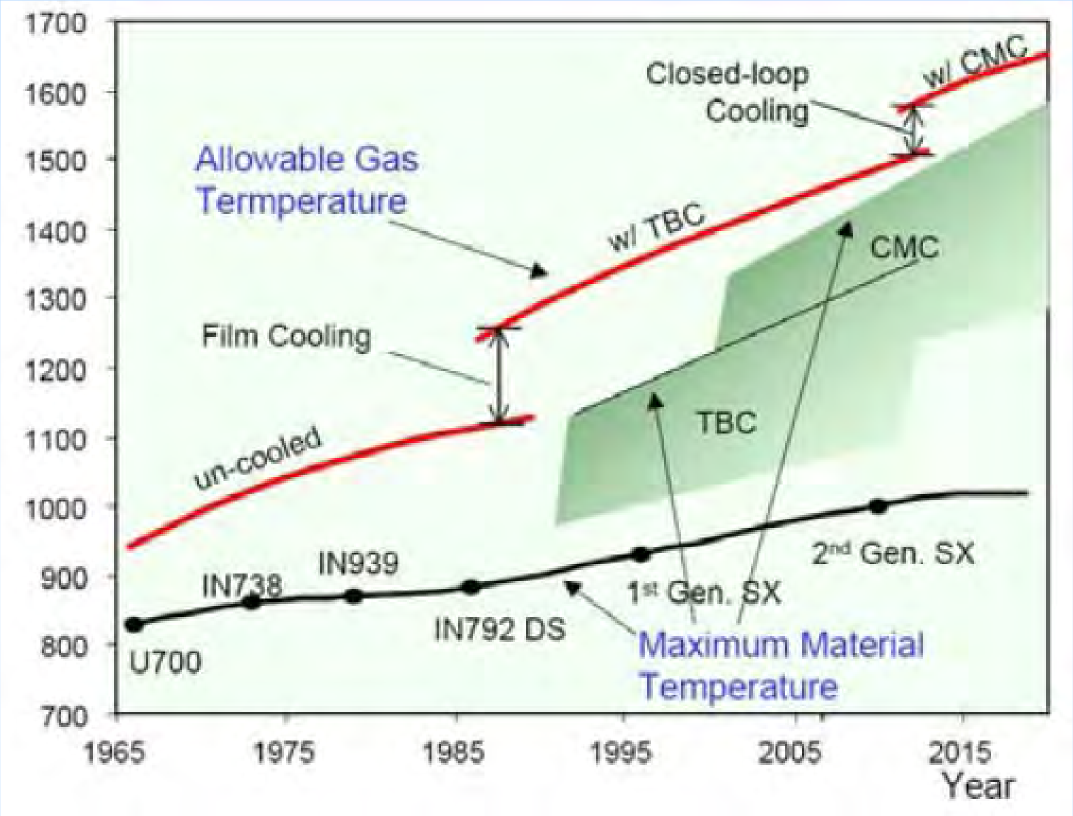

- **Higher temperature capability**
- **High corrosion resistance**
- **Toughening mechanisms:**
  - **- Microcracking**
  - **- Fiber pull out**
  - **- Crack bridging**
- **90% cooling air reduction**
- **Reduced emissions**

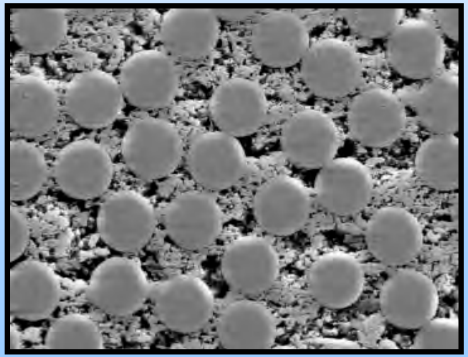

D. R. Clarke, Harvard University, Jan 2015

Future Limits To Gas Turbines: Unresolved Challenges

- Atmospheric pollution from engine exhausts
  - Chemical reactions produce NOx -- will limit max combustion temperature

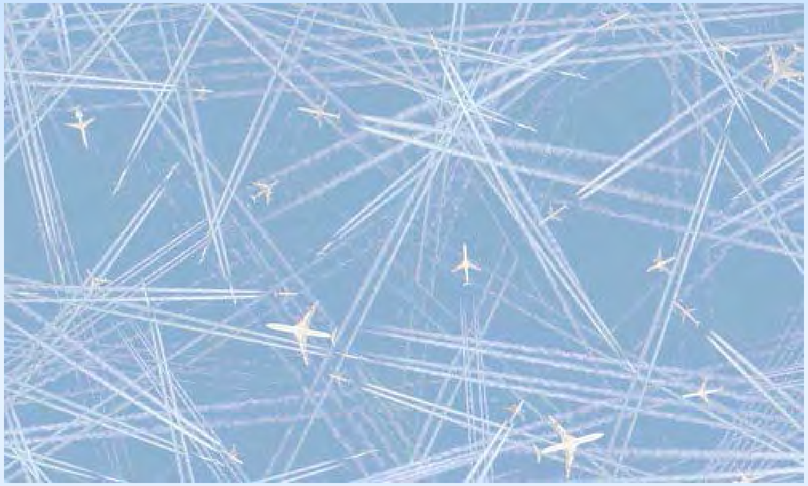

- Melting of ingested sand can erode TBC -- CMAS
- Corrosion of metallic components from pollution in the atmosphere, eg SO_2
  - Many of the metallic alloys in the engine were not designed to resist SO_2 corrosion

NOx Emissions Depend on Combustion Temperature

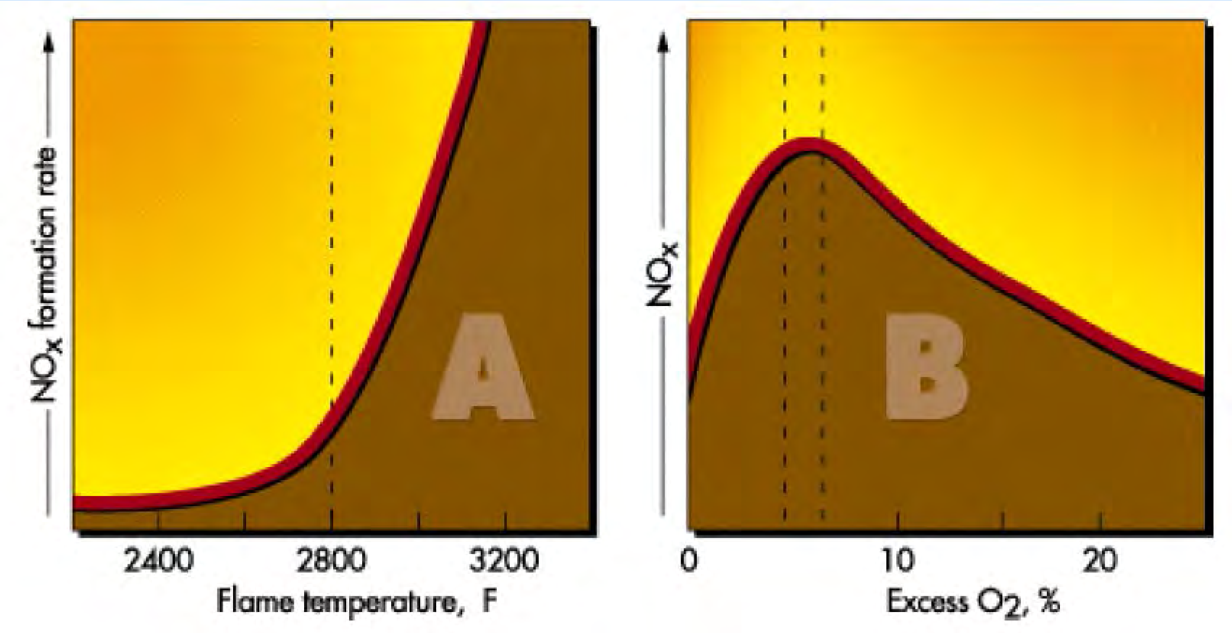

On land-based turbines, *NOx* can be reduced by steam injection into combustor

Aerospace turbines might need their own high-temperature catalytic convertor

SO_2 Corrosion Resistance

Growing problem: rising SO2 levels in air in many cities around the world

Probably will require extensive modification of bond-coat alloys.

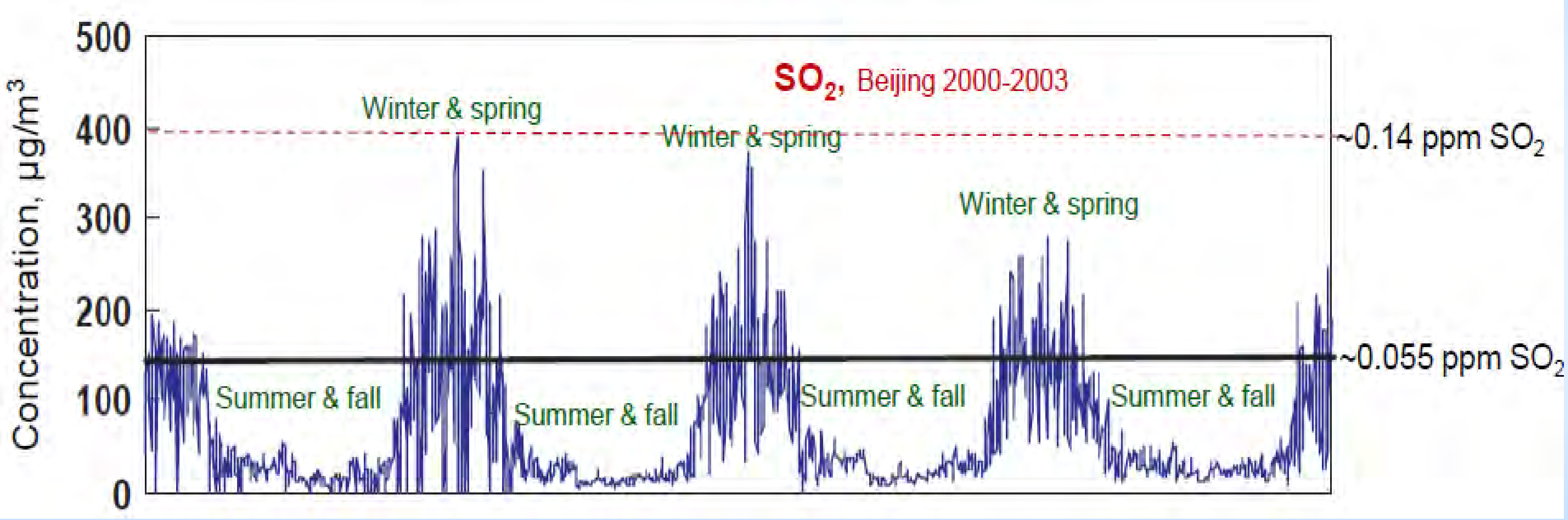

SO_2 Corrosion Resistance

Growing problem: rising SO2 levels in air in many cities around the world.
Current bond-coat alloys were designed for much lower SO2 levels.
Solution: probably will require extensive modification of bond-coat alloys.

Source: R. Sokhi, World Atlas of Atmospheric Pollution, Anthem Press, New York, 2008

D. R. Clarke, Harvard University, Jan 2015

Summary and Future Directions

Identifying the next generation thermal barrier coatings remains a major challenge

- Low thermal conductivity at high temperatures is a *necessary but not sufficient* criterion.
- Thermal conductivity at low temperatures is relatively un-important and not a good guide to high-temperature conductivity
- High fracture toughness at high temperatures is also a necessary requirement.
- Thermal barrier coatings are part of a dynamically evolving and interacting system.
- Bond-coat and superalloy must also be morphologically stable, especially on thermal cycling

Future Directions

- Development of *in-situ* monitoring, particularly of coating temperatures and damage.
- Operation in air containing higher SO2 concentrations.
- Coatings for turbines using alternative fuels.
- Plenty of inter-disciplinary research and development opportunities
- Success will require a large scale, multidisciplinary approach and extensive collaborations

Acknowledgements

- Office of Naval Research, Steve Fishman and Dave Shifler
- Vladimir Tolpygo, Andi Limarga, Molly Gentleman, Sam Shian, Yang Shen,
- Vanni Lughi, Liguo Chen, Matthew Chambers, John Nychka, Mary Gurak
- Professors Carlos Levi and Tony Evans, UC Santa Barbara
- Ken Murphy, Howmet Research Center, ALCOA
- Mike Maloney, Pratt and Whitney
- Ram Darolia, GE Aviation, Don Lipkin, GE Corporate Research
- Vladimir Tolpygo and Wil Baker, Honeywell Aviation
- Bauke Heeg, Luminium

Want to Know More ?

Edited: Clarke, Oechsner, Padture

clarke@seas.harvard.edu